

FINAL REPORT

Advanced Monitoring of Migratory Birds on Military Lands

SERDP Project RC-1438

MARCH 2010

Anna M. Pidgeon
University of Wisconsin-Madison

This document has been cleared for public release



Report Documentation Page

Form Approved
OMB No. 0704-0188

Public reporting burden for the collection of information is estimated to average 1 hour per response, including the time for reviewing instructions, searching existing data sources, gathering and maintaining the data needed, and completing and reviewing the collection of information. Send comments regarding this burden estimate or any other aspect of this collection of information, including suggestions for reducing this burden, to Washington Headquarters Services, Directorate for Information Operations and Reports, 1215 Jefferson Davis Highway, Suite 1204, Arlington VA 22202-4302. Respondents should be aware that notwithstanding any other provision of law, no person shall be subject to a penalty for failing to comply with a collection of information if it does not display a currently valid OMB control number.

1. REPORT DATE

MAR 2010

2. REPORT TYPE

3. DATES COVERED

00-00-2010 to 00-00-2010

4. TITLE AND SUBTITLE

Advanced Monitoring of Migratory Birds on Military Lands

5a. CONTRACT NUMBER

5b. GRANT NUMBER

5c. PROGRAM ELEMENT NUMBER

6. AUTHOR(S)

5d. PROJECT NUMBER

5e. TASK NUMBER

5f. WORK UNIT NUMBER

7. PERFORMING ORGANIZATION NAME(S) AND ADDRESS(ES)

University of Wisconsin-Madison, 500 Lincoln Dr, Madison, WI, 53706

8. PERFORMING ORGANIZATION
REPORT NUMBER

9. SPONSORING/MONITORING AGENCY NAME(S) AND ADDRESS(ES)

10. SPONSOR/MONITOR'S ACRONYM(S)

11. SPONSOR/MONITOR'S REPORT
NUMBER(S)

12. DISTRIBUTION/AVAILABILITY STATEMENT

Approved for public release; distribution unlimited

13. SUPPLEMENTARY NOTES

14. ABSTRACT

Department of Defense natural resource managers need information on where specific bird species of conservation concern are most likely to occur, and where hotspots of migratory species richness are located, in order to successfully implement installation-specific Integrated Natural Resource Management Plans. In this project, the research team developed an approach to characterizing the patterns of presence and abundance of bird species in open-canopy ecosystems. The approach integrates landscape level analysis with spatially detailed habitat information, using remotely sensed image texture which is derived from unclassified imagery. We calculated image texture from digital aerial photos, from Landsat Thematic Mapper satellite imagery which provides data on individual bands of the electromagnetic spectrum, and from a derived product, the Normalized Difference Vegetation Index. In the Chihuahuan Desert ecosystem of Fort Bliss, NM, Normalized Difference Vegetation Index alone accounted for up to 82% of the variability in species richness, while image texture derived from aerial photos was the strongest single predictor of species richness (capturing 52% of variation) in the grasslandsavanna- woodland ecosystem of Fort McCoy, WI. Maps of avian abundance and occurrence were developed from models using image texture at both installations. The mapping effort revealed that texture measures account for variability within landcover classes, reflecting finescale patterns of species abundance and occurrence that are not apparent in maps based on models using landcover class data only, while retaining a broad-extent perspective. In the Fort McCoy ecosystem, the near-infrared band from Landsat Thematic Mapper imagery accounted for 74% of ground-measured vertical vegetation structure, which is strongly associated with bird distribution patterns. In a focal study on Fort Bliss of the Loggerhead Shrike, a species of conservation concern, models based on local (i.e. ground measured) and intermediate-scale (i.e. image texture) but not broad scale (i.e. land cover class) habitat variables best explained Shrike occurrence. Finally, the research group conducted an analysis of phenological variation of texture measures in three North American biomes, and found that interseasonal variability is strong, which both offers opportunities and presents challenges. The degree to which texture measures were robust to seasonality and scale of analysis was quantified. In summary, image texture is a useful measure in models of habitat. Models based on image texture performed equal to or better than models based on classified habitat maps for characterizing habitat use by birds across broad extents. This project has highlighted the potential to integrate remotely sensed measures of habitat structure in habitat models.

15. SUBJECT TERMS

16. SECURITY CLASSIFICATION OF:

a. REPORT
unclassified

b. ABSTRACT
unclassified

c. THIS PAGE
unclassified

17. LIMITATION OF
ABSTRACT
**Same as
Report (SAR)**

18. NUMBER
OF PAGES
54

19a. NAME OF
RESPONSIBLE PERSON

This report was prepared under contract to the Department of Defense Strategic Environmental Research and Development Program (SERDP). The publication of this report does not indicate endorsement by the Department of Defense, nor should the contents be construed as reflecting the official policy or position of the Department of Defense. Reference herein to any specific commercial product, process, or service by trade name, trademark, manufacturer, or otherwise, does not necessarily constitute or imply its endorsement, recommendation, or favoring by the Department of Defense.

Table of Contents

| | |
|--|----|
| Abstract..... | 1 |
| Objectives | 2 |
| Background..... | 3 |
| Materials and Methods | 6 |
| Collection of field data..... | 7 |
| Testing the relationship between foliage height diversity and image texture at Fort McCoy..... | 10 |
| The role of remotely sensed data in accounting for avian patterns at Fort Bliss and Fort McCoy | 12 |
| Analysis of the impact of phenological variation on texture measures. | 15 |
| Results and Discussion..... | 16 |
| The relationship between foliage height diversity and image texture at Fort McCoy..... | 16 |
| Bird Species richness models | 17 |
| Species distribution models and maps of predicted probability of occurrence and abundance ... | 24 |
| The impact of phenological variation on texture measures. | 37 |
| Conclusions and Implications for Future Research | 39 |
| Literature Cited | 40 |
| Appendix A – supporting material..... | 43 |
| Appendix B – List of Scientific/Technical Publications | 47 |

List of Tables

| | |
|---|----|
| Table 1: Eight second-order measures of image texture, calculated from a gray-level co-occurrence matrix (GLCM) ordered by texture group, with description of what they measure, and the statistic formula. | 11 |
| Table 2. Results from univariate linear regression models relating species richness to single image texture at different moving window sizes. | 18 |
| Table 3. Range of R2adj, BIC, and σ PRESS values for the Fort Bliss species richness models used to obtain posterior probabilities using the Bayesian Model Averaging (BMA) approach. | 20 |
| Table 4. Fort McCoy species richness models. | 23 |
| Table 5. Validation of probability of occurrence maps, Fort Bliss. | 29 |
| Table 6. Mean density of birds at Fort McCoy. | 31 |
| Table 7. Loggerhead Shrike on Fort Bliss: the spatial scales at which habitat was assessed, that best explained occurrence of adults and nests. | 33 |
| Table 8. Fort McCoy models of abundance. | 34 |

List of Figures

| | |
|--|----|
| Figure 1. Three major factors influencing species richness (MacArthur 1972). | 3 |
| Figure 2. Location of the two study sites. | 4 |
| Figure 3. Digital aerial photos of A) black grama grassland, B) sandsage, and C) mequite habitat. | 6 |
| Figure 4. Illustration of digital numbers and grey-level oc-occurrence matrix. | 6 |
| Figure 5. Landsat satellite image of McGregor Range of Fort Bliss, NM, indicating location of bird surveys. | 7 |
| Figure 6. Images of representative habitats, Fort Bliss. | 8 |
| Figure 7. Images of representative habitats, Fort McCoy. | 9 |
| Figure 8. Airphoto image of Fort McCoy, WI. | 9 |
| Figure 9. Scatterplots of vegetation structure variables vs. image texture values. | 17 |
| Figure 10. Scatterplots of predicted density of Grasshopper Sparrow at 32 grassland sample plots, Field Sparrow at 82 savanna plots, and Ovenbird at 52 woodland sample points, and bird species richness at 166 sample plots versus texture measures. | 22 |
| Figure 11. Predicted abundance of three species on McGregor Range of Fort Bliss. | 24 |
| Figure 12. Predicted abundance of three additional species on McGregor Range of Fort Bliss. | 25 |
| Figure 13. Predicted probability of occurrence of three bird species on McGregor Range, Fort Bliss. | 26 |
| Figure 14. Predicted probability of occurrence of six more bird species on McGregor Range, Fort Bliss. | 27 |
| Figure 15. Maps of predicted species abundance were validated by comparing counts predicted at 42 new study plots (“test data” in figure, obtained in 2006 – 2008) against counts obtained in 1996-1998 at 42 original plots (“model data” in figure). | 28 |
| Figure 16. Maps of predicted average abundance of three species at Fort McCoy, WI. | 37 |
| Figure 17 Mean image-wide coefficient of variation of first-order texture measures averaged across bands and three window sizes, for three study sites (New Mexico, Ontario, and Virginia). | 38 |
| Figure 18. Mean image-wide coefficient of variation averaged across bands and three window sizes for each study site. | 38 |

List of Acronyms

| | |
|-------|---|
| AUC | Area under the relative operating characteristic curves |
| BMA | Bayesian Model Averaging |
| ESA | Endangered Species Act |
| GLCM | Gray level co-occurrence matrix |
| INRMP | Integrated Natural Resource Management Plan |
| MBTA | Migratory Bird Treaty Act |
| MSE | Mean Square Error |
| NDVI | Normalized difference vegetation index |
| NIR | Near Infrared band of the electromagnetic spectrum |
| TM | Thematic Mapper |

Bird Species:

| | |
|------|------------------------|
| BRSP | Brewer's Sparrow |
| BTSP | Black-throated Sparrow |
| BLGR | Blue Grosbeak |
| CAKI | Cassin's Kingbird |
| CONI | Common Nighthawk |
| EAME | Eastern Meadowlark |
| GTTO | Green-tailed Towhee |
| LASP | Lark Sparrow |
| LENI | Lesser Nighthawk |
| SCOR | Scott's Oriole |
| WEKI | Western Kingbird |
| WIWA | Wilson's Warbler |

Key Words

Image texture, remote sensing, birds, species richness, abundance, presence, vegetation, structure, habitat, model, Chihuahuan Desert, grassland, savanna, woodland, NDVI, aerial photo, satellite image

Acknowledgements

I gratefully acknowledge support by the Strategic Environmental Research and Development Program. Acquisition of bird data was supported by the U.S. Department of Defense Legacy Resource Management Program, Ft. Bliss Directorate of Environment, Fort McCoy Directorate of Public Works, USGS BRD Texas Cooperative Fish and Wildlife Research Unit, USGS BRD Wisconsin Cooperative Wildlife Research Unit, and the Department of Wildlife Ecology at the University of Wisconsin–Madison. Dr. Veronique St-Louis and Mr. Eric Wood (anticipated graduation date May 2011), the two PhD students who spearheaded the field work and conducted statistical analyses leading to the results found in this report, made the most of the opportunities and the challenges of this project, and did excellent work. I especially appreciate the assistance

of Dr. Brian Locke and Mr. Dallas Bash at Fort Bliss, and the assistance of Mr. Tim Wilder, Mr. David Beckmann, Ms. Sue Vos, Dr. Kim Mello (retired) and Mr. David Asleysan at Fort McCoy. I also appreciate the insights of Drs. Volker Radeloff, Murray Clayton, Claudio Grattin, Randy Jackson, Christine Ribic, David Mladenoff, Phil Townsend, who participated as advisors on the PhD committees of Veronique St-Louis and Eric Wood.

Abstract

Department of Defense natural resource managers need information on where specific bird species of conservation concern are most likely to occur, and where hotspots of migratory species richness are located, in order to successfully implement installation-specific Integrated Natural Resource Management Plans. In this project, the research team developed an approach to characterizing the patterns of presence and abundance of bird species in open-canopy ecosystems. The approach integrates landscape level analysis with spatially detailed habitat information, using remotely sensed image texture which is derived from unclassified imagery. We calculated image texture from digital aerial photos, from Landsat Thematic Mapper satellite imagery which provides data on individual bands of the electromagnetic spectrum, and from a derived product, the Normalized Difference Vegetation Index. In the Chihuahuan Desert ecosystem of Fort Bliss, NM, Normalized Difference Vegetation Index alone accounted for up to 82% of the variability in species richness, while image texture derived from aerial photos was the strongest single predictor of species richness (capturing 52% of variation) in the grassland-savanna-woodland ecosystem of Fort McCoy, WI. Maps of avian abundance and occurrence were developed from models using image texture at both installations. The mapping effort revealed that texture measures account for variability *within* landcover classes, reflecting fine-scale patterns of species abundance and occurrence that are not apparent in maps based on models using landcover class data only, while retaining a broad-extent perspective. In the Fort McCoy ecosystem, the near-infrared band from Landsat Thematic Mapper imagery accounted for 74% of ground-measured vertical vegetation structure, which is strongly associated with bird distribution patterns. In a focal study on Fort Bliss of the Loggerhead Shrike, a species of conservation concern, models based on local (i.e. ground measured) and intermediate-scale (i.e. image texture) but not broad scale (i.e. land cover class) habitat variables best explained Shrike occurrence. Finally, the research group conducted an analysis of phenological variation of texture measures in three North American biomes, and found that interseasonal variability is strong, which both offers opportunities and presents challenges. The degree to which texture measures were robust to seasonality and scale of analysis was quantified. In summary, image texture is a useful measure in models of habitat. Models based on image texture performed equal to or better than models based on classified habitat maps for characterizing habitat use by birds, across broad extents. This project has highlighted the potential to integrate remotely sensed measures of habitat structure in habitat models.

Objectives

Department of Defense natural resource managers need information on where specific migratory bird species are most likely to occur, and where hotspots of migratory species richness are located, in order to implement improved mitigation procedures that protect migratory bird species without degrading realistic military training. Accurate environmental risk assessments that comply with the Migratory Bird Treaty Act (MBTA) and the Endangered Species Act (ESA) require detailed information on the patterns of species presence and species abundance. Installation Integrated Natural Resource Management Plans (INRMPs) are useful to the degree that they are based on information about patterns of distribution of species of interest, at relevant scales. The aim of this project was to develop a migratory bird monitoring strategy for military lands that integrates field based monitoring with satellite image analysis, and to address manager's needs for broad scale, but relatively detailed maps of individual species occurrence and 'hotspots' of species richness.

Initial development of this idea evolved from the observation that species richness within the desert bird community of Fort Bliss responded to foliage height diversity positively, a relationship initially articulated by MacArthur and MacArthur (1961), and which has been found to hold true in many other habitat types. Our working hypothesis was that 1) there is a strong positive relationship between foliage height diversity and remotely sensed image texture, a measure of habitat heterogeneity, and 2) image texture has the same positive relationship with bird species richness that foliage height diversity does, and the two measures are likely to be interchangeable in models of bird habitat.

The overarching goals of this project were therefore to identify the fundamental relationship of habitat elements that define migratory landbird habitat in desert and savanna environments, to develop texture-based image processing methods for satellite and airphoto data to forecast migratory bird distribution and abundance, and to generalize these forecasting methods to other ecosystems.

The project had four major objectives:

- Determine the relationship of migratory bird presence and abundance to habitat structure in desert environments as depicted in the image texture of airphotos and satellite data
- Test the reliability of these relationships using an existing dataset of migratory bird presence and abundance
- Predict abundance and presence of migratory birds based on these habitat measures at a fine-scale across entire military installations
- Use the results of these desert- based findings to inform prediction of abundance and presence of migratory birds in a prairie – savanna ecosystem.

Background

Understanding the spatial and temporal pattern of species and populations has been a major goal of ecological research since the beginnings of the field (e.g., Grinnell 1917). A rich theory of habitat selection developed that sought to explain how individuals within a population are distributed among limited habitat resources. Biodiversity is generally related to three broad factors: habitat structure, climatic stability, and productivity (Figure 1; MacArthur 1972). Specific structural aspects of habitat are good predictors of bird diversity and of occupancy by certain species (MacArthur and MacArthur 1961). Vegetation structure may be a good predictor of occurrence and therefore of species richness (i.e. number of species found at a given site) because it may function as an indicator of foraging sites, insect density, or other aspects of foraging and food supply for birds (Cody 1981). Competition can modify habitat selection, so that if the dominant competition is primarily from within a species, the range of habitats occupied by a species expands, while if the dominant competition is from other species, a species' range contracts (Svardson 1949). This phenomenon, and density-dependent habitat use generally, is well documented and is the subject of several explanatory theories (MacArthur and Levins 1964, Fretwell and Lucas 1970, Rosenzweig 1981).

The importance of habitat availability for the distribution patterns of wildlife allows prediction of their abundance via habitat mapping. Remotely sensed imagery is a prime data source for broad scale habitat mapping and its earliest uses for this purpose date back three decades (Reeves et al. 1976, Laperriere et al. 1980). Satellite imagery has been the basis of predictions of single species distributions (Aspinall and Veith 1993) and patterns of biodiversity (Stoms and Estes 1993, Griffiths et al. 2000, Luoto et al. 2002, Turner et al. 2003). The common approach is to conduct a pixel-by-pixel classification using the reflectance values in multi-channel imagery to identify vegetation classes (Lillesand and Kiefer 2004). Species distribution patterns are statistically modeled by integrating wildlife survey plot data with the satellite image classification (Fuller et al. 1998). This approach has been used for many species, ranging from Black-throated Sparrow (*Amphispiza bilineata*, Pidgeon et al 2003) to Wood Stork (*Mycteria americana*, Hodgson et al. 1987, 1988), and groups of multiple species have been modeled in geographically distinct areas ranging from Maine (Hepinstall and Sader 1992), to the Greater Yellowstone Ecosystem (Saveraid et al. 2001), and Polynesia (Franklin and Steadman 1991).

In addition to the type, structure, and availability of habitat, the *scale* at which these elements are considered is important. Military installations, in particular, are often vast in extent. Therefore, models of habitat use that are relevant only to local areas are of limited use to natural resource managers responsible for implementing INRMPS. Patterns and processes operating at the landscape scale are a crucial factor influencing species distributions (Turner et al. 1989). Population ecologists have demonstrated that species distributions can be determined by metapopulation dynamics (Flather and Bevers 2002) or source-sink dynamics (Pulliam 1988). Landscape indices depicting fragmentation (e.g., patch size and patch isolation, Turner 1989) are powerful determinants of migratory bird presence and abundance in landscapes that are forested

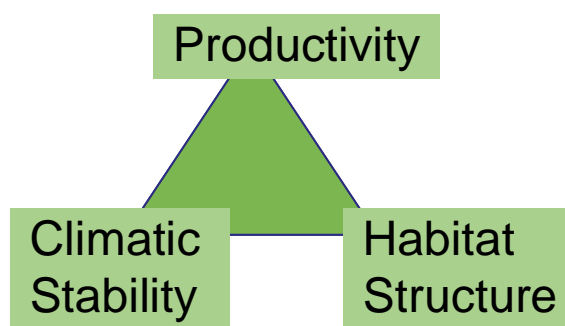


Figure 1. Three major factors influencing species richness (MacArthur 1972).

(Flather and Sauer 1996, Trzcinski et al. 1999) or agriculturally dominated (Herkert 1994, Bergin et al. 2000).

Taken together, the information from these and other studies suggested that pixel-by-pixel habitat classification should be combined with landscape level habitat analysis when predicting

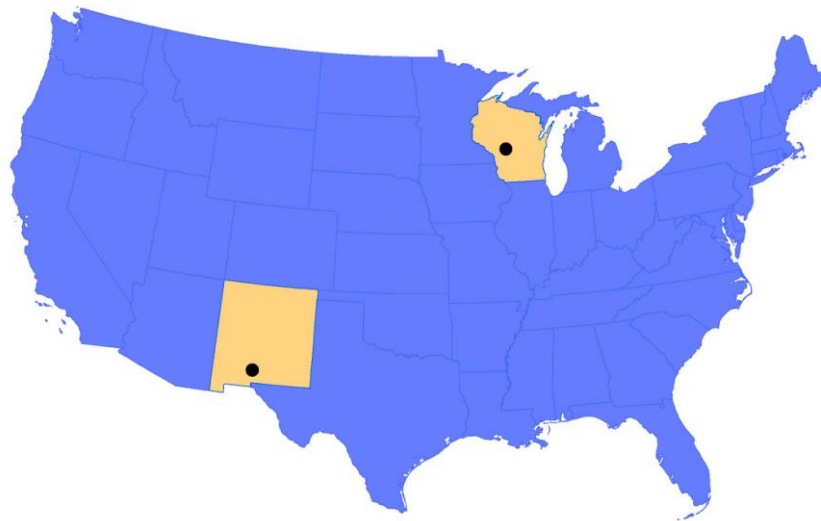


Figure 2. Location of the two study sites. Fort Bliss is within the Chihuahuan Desert Province in southern New Mexico. Fort McCoy is within the Eastern Broadleaf Forest (Continental) province (Bailey 1995).

bird distribution and abundance, and that this integrated approach should play a key role in an advanced monitoring strategy for migratory birds on military lands.

However, in order to apply this successfully across military installations in the U.S., another issue needed to be considered.

The majority of all military land is located in deserts (70%) while satellite-based habitat mapping has largely focused on forested and/or human dominated (i.e. agricultural) landscapes.

The results of field-based studies show that bird species composition in deserts is influenced by vegetation differences, such as contrasts between desert riparian and desert scrub habitat (Szaro and Jakle 1985, Naranjo and Raitt 1993, Kozma and Mathews 1997), and grazed versus ungrazed areas (Gonnet 2001, Krueper et al. 2003). Presence of avian granivores in desert grasslands is influenced by the availability of vegetation that functions as an escape from predators (Lima and Valone 1991). In general, avian presence and species diversity are consistently found to be related to vegetation based habitat measures, such as foliage height diversity (Tomoff 1974, Mills et al. 1989, Imhoff et al. 1997, Pidgeon et al. 2001).

However, mapping habitat elements that birds respond to in desert or ecotonal environments, such as a prairie-savanna mosaic, using traditional pixel-by-pixel habitat classification methods, poses a problem. By definition, a habitat classification obscures subtle variation within one habitat, such as the density of shrubs available for nesting, which can be a key determinant of migratory bird presence and abundance (Pidgeon et al. 2001). Traditional pixel-by-pixel habitat classification methods are not suitable to detect within-habitat variation, and bird abundance maps resulting from this are relatively coarse and do not capture potentially important within-habitat variability (e.g., Pidgeon et al 2003).

Another problem is related to the use of landscape level habitat measures in desert or savanna environments. Initial research that has been done shows that landscape level factors (i.e. number of patches) are important for avian habitat quality in desert environments (Gutzwiller and Barrow 2002). The problem is that all commonly used landscape indices require a basemap of distinct habitat types. This makes sense in human dominated landscapes with discrete patches, but desert and savanna environments rarely exhibit distinct patch boundaries. Instead, transitions

among habitat types occur along gradients (Imhoff et al. 1997, Asner et al. 2000). For example, in the Chihuahuan Desert where one half of this study is based, patch boundaries are ‘soft’, either because the vegetation is structurally similar (e.g., between creosotebush and whitethorn acacia- habitats) or because there is a broad ecotone between habitat types (e.g., between sandsage and mesquite, or whitethorn and black grama). In the prairie-savanna ecosystem, the density of shrubs and trees in prairies and savannas depends on fire and disturbance history, and forms a broad ecotone as well. Consequently, commonly used landscape indices (Turner 1989) are not well suited for predicting migratory bird distribution and abundance in desert and savanna environments. These challenges made clear the need for new and improved methods for mapping avian habitat at sufficient detail to reflect avian patterns of use, and at a broad enough scale that management strategies could be planned and implemented. We elected to explore the use of image texture measures to characterize migratory bird habitat. At the time we proposed this project there had been success in applying image texture to vegetation classifications, but only one study that had used image texture to map wildlife habitat explicitly. Hepinstall and Sader (1997) predicted the probability of occurrence for 14 species of Maine land birds using spectral values of 30 m Landsat TM imagery and derived texture measures. Based on their results, we investigated texture measures from airphotos and Landsat TM imagery and their application to predicting bird patterns at Fort Bliss, and then at Fort McCoy (Figure 2).

Materials and Methods

The approach we proposed combined existing field based data on bird distribution and abundance with remotely sensed data, using advanced image processing methods to identify image correlates of environmental features that predict bird presence and abundance.

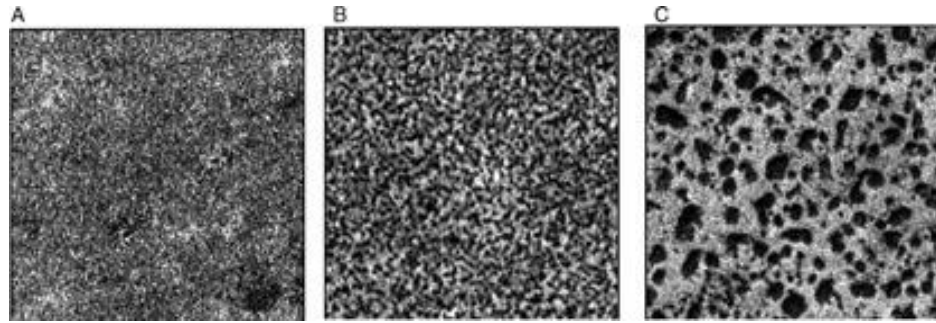


Figure 3. Digital aerial photos of A) black grama grassland, B) sandsage, and C) mequite habitat.

The novelty of our approach centers on the use of image texture. Image texture is calculated on unclassified imagery, which retains all of the heterogeneity available in the particular pixel resolution and amount of the electromagnetic spectrum captured in a given remotely sensed (i.e. satellite- or fixed wing aircraft-based) data source (e.g., Figure 3). Image texture measures the heterogeneity in tonal values (i.e., digital numbers, which represent brightness) within a defined

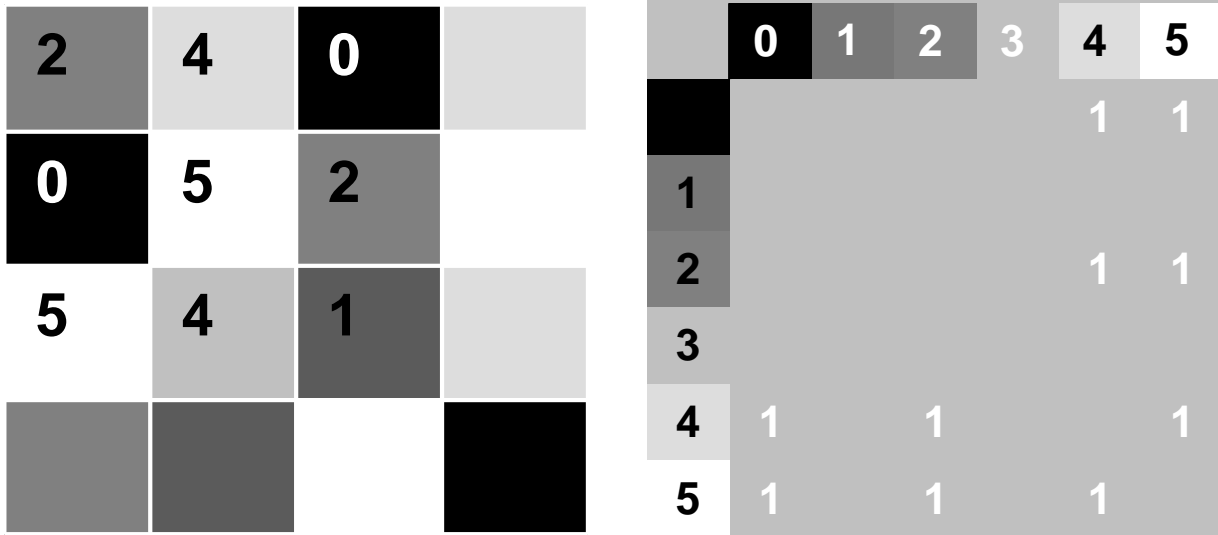


Figure 4. Illustration of digital numbers and grey-level co-occurrence matrix. Left: Example of pixel digital numbers in a 3 x 3 window. First-order statistics are calculated directly on these numbers. Second-order statistics are calculated on a grey-level co-occurrence matrix (Right) that calculates the number of co-occurrences of pairs of pixel values in a four directions (0°, 45°, 90°, and 135°), and averaged (Haralick 1973).

area of an image. Some images are dominated by tone (homogenous digital numbers throughout an image) whereas others are dominated by texture (heterogenous digital numbers across an image, Haralick et al. 1973, Haralick 1979). The most commonly used measures of texture are divided into two groups: first-order (occurrence) and second-order (co-occurrence). First-order measures are statistics calculated from the spectral values of pixels in a defined neighborhood, typically implemented as a moving window. Common first-order measures include minimum, maximum, range, mean, standard deviation, skewness, and kurtosis. Second-order texture

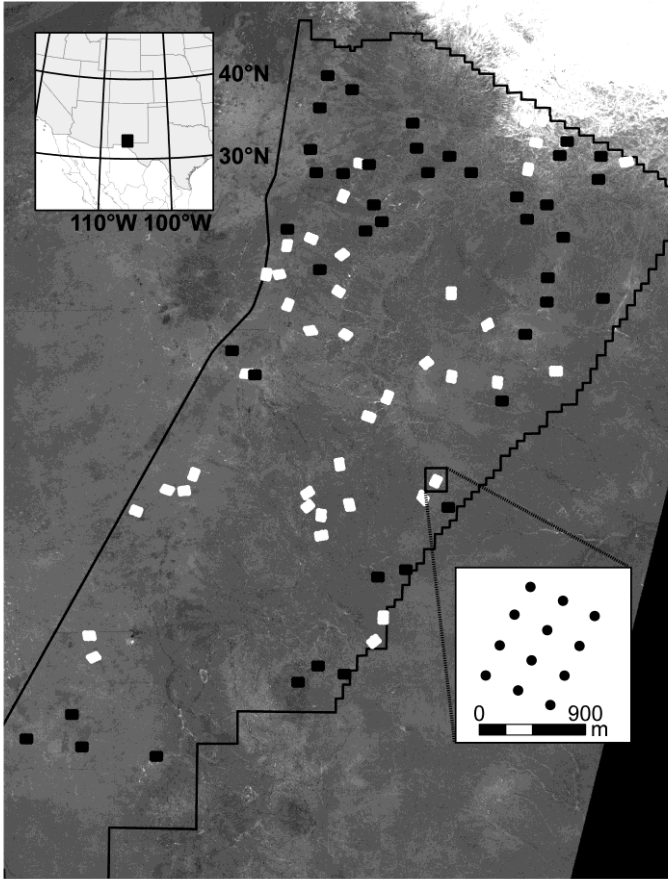


Figure 5. Landsat satellite image of McGregor Range of Fort Bliss, NM, indicating location of bird surveys. White dots indicate location of 42, 108 ha plots surveyed for bird species richness and abundance data from 1996-1998. Black dots indicate location of 42 independent plots surveyed 2006-2008 that were used to test models developed from the 1990s data.

Mexico, where we had previously collected a three year data set of bird distribution (Figure 5). The project was subsequently expanded to Fort McCoy, Wisconsin. Both of these sites have open canopy vegetation structure, and we felt they would provide a good opportunity to test of the usefulness of image texture for bird habitat analysis in a range of open-habitat environments.

Fort Bliss is located in the northern Chihuahuan Desert. McGregor Range of Fort Bliss encompasses approximately 282,500 ha, and includes seven major habitat types, including, at the lowest elevation (1200 m) on the west half of the Range, three shrub-dominated habitat types; sandsage, mesquite and creosotebush. Moving up in elevation, another shrub-dominated habitat type, whitethorn acacia is found, and moving up in elevation, it intergrades with black grama grassland. At about 1800 m, mesa grassland dominates and ranging to 2400 m, pinyon-juniper covers the northern part of the Range.

measures take into account the spatial distribution of spectral values, and are derived from the gray-level co-occurrence matrix (Figure 4). Entries in the matrix represent the relative frequency of pixels with tone levels and co-occurring at a user specified distance (typical distance is 1 pixel) and direction. Image texture offers promise as a measure useful for analyses that are fine grained, yet broad in extent, a combination of attributes that are necessary for effective landscape-scale characterization of avian habitat structure. Additionally, because calculation of image texture measures does not rely on a landcover classification, which is often labor-intensive to produce, its use in habitat models is cost-effective relative to models based on landcover classifications. We tested both individual measures of texture and the effect of scale, as represented by calculating texture in different window sizes.

Collection of field data

We conducted the initial phase of work on McGregor Range of Fort Bliss, located primarily in New



Figure 6. Images of representative habitats, Fort Bliss. Clockwise from top left: mesquite dunes, cressosote-bush, pinyon-juniper, and black-grama grassland.

For the Fort Bliss analysis, we used existing avian data that had been collected during the breeding season (late April to May) of 1996 to 1998 to build statistical models and to make species abundance/occurrence maps, and used data collected during the breeding seasons of 2006-2008 to test the validity of the models and maps. In each period, 42 plots were sampled. In the first time period, 6 plots were randomly placed in each of 7 habitat types. In the second time period, 7 plots were placed in each of 6 image texture categories, spanning the image texture range encompassed by the first set of plots. Each study plot consisted of a 12-point grid (3 x 4) with points located 300 m apart, so that each plot encompassed 108 ha. We collected data on bird presence and abundance using 10-minute point counts following standard methods for that time period (Ralph et al 1995, Pidgeon et al 2001). Plots were visited four times each year in the first set of plots, and twice each year in the second set of plots, and all birds detected within 150 m at each of the twelve points were tallied by species.

At Fort McCoy we collected data on habitat and avian distribution in the the grassland-savanna- woodland mosaic (Figure 7). The areas of Fort McCoy available to us for study were interspersed with off-limits training areas and roads, and required a different sampling design than was used at Fort Bliss. Survey points for collecting data on birds were distributed among grassland (n=50), black oak (*Quercus velutina*) savanna (n=91), and woodland habitat (n=65; Figure 8). Each survey point was surrounded by at least 100 m of homogeneous habitat (grassland, savanna, or woodland), and was at least 100 m from roads. At each survey point we

conducted 10-minute point counts in 2007-2009 to estimate bird abundance, by species, following standard methods that now include estimate of distance to each individual bird, so that detectability differences can be accounted for in later calculations of abundance.



Figure 7. Images of representative habitats, Fort McCoy. Left to right; short grass prairie, black oak savanna, red and black oak woodland.

Each survey point is the center of a 100 m radius plot, and once during the three year period we sampled habitat structure in each plot. We sampled foliage height diversity (MacArthur and MacArthur 1961, Wiens and Rotenberry 1981), using a 12 m tall pole marked at 30 cm intervals. At each sample point, four sub-plots were selected where measurements were collected. One sub-plot was located at the center of the sample point, and the three remaining sub-plots were located at a random distance between 20 m and 80 m, with one in each compass direction: 0°, 120°, 240°. From the center point of each sub-plot, one observer walked 5 m in each of the cardinal directions and placed the pole vertically on the ground. A second observer recorded all hits (i.e., instances where vegetation touched the pole) per 30 cm segment. If the canopy was taller than 12 m, the second observer used binoculars to estimate vegetation hits at approximate 30 cm intervals. This yielded four measurements at each of the four sub-plots totaling 16

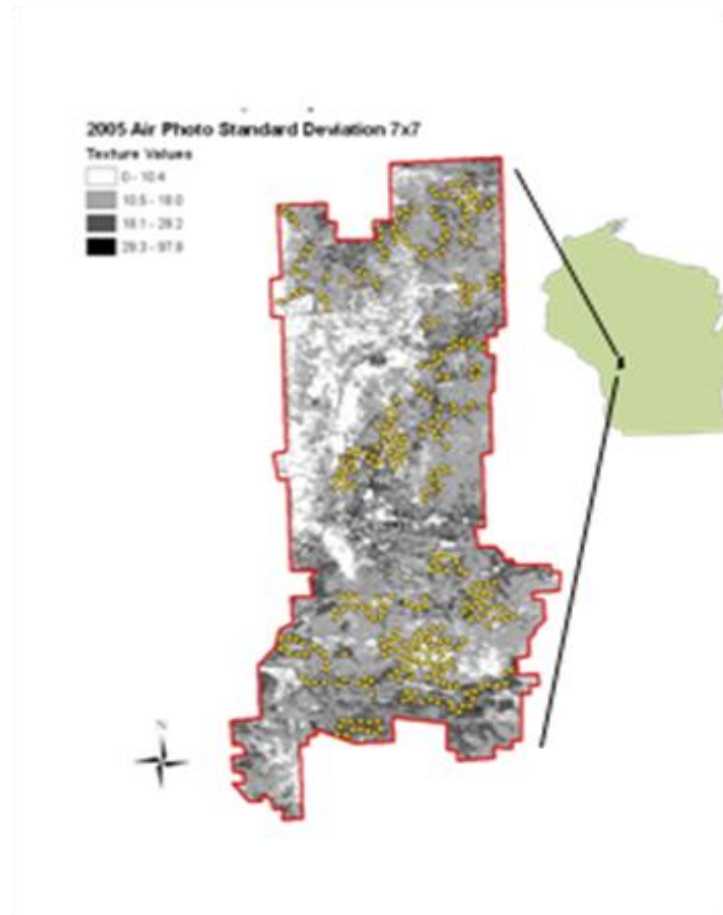


Figure 8. Airphoto image of Fort McCoy, WI. Yellow dots indicate location of 206, 100 m radius plots at which bird species richness and abundance data were collected in 2007-2009.

foliage-height profile measurements at each plot.

From these 16 foliage-height diversity measurements, three indices of vegetation structure were calculated. First, an index of vertical structure, called foliage height diversity, was computed (MacArthur and MacArthur 1961). Second, a horizontal vegetation structure index was derived by taking the standard deviation of the highest intersection of vegetation on the pole at the 16 foliage-height diversity measurements per sample point (Wiens and Rotenberry 1981). Third, a foliage volume index was derived by summarizing the total number of hits of vegetation along the pole at a sample point, from the 16 pooled foliage-height diversity measurements (Estades 1997).

Testing the relationship between foliage height diversity and image texture at Fort McCoy

We know from previous work that in the Northern Chihuahuan Desert ecosystem of McGregor Range of Fort Bliss the relationship between bird species richness and foliage height diversity is positive (Pidgeon 2000), consistent with findings in many other ecosystems (Karr and Roth 1971, Rotenberry and Wiens 1980, Wiens and Rotenberry 1981, Rosenzweig 1995, Patterson and Best 1996, Estades 1997), and the relationship between image texture and foliage height diversity is positive (Pidgeon, unpublished data). We were unsure of the direction of these relationships in the grassland-savanna-woodland mosaic at Fort McCoy, and therefore we initially tested the relationship between foliage height diversity and image texture.

An infrared air photo (~ 1 m resolution) from August 2006 and a Landsat TM (hereafter Landsat) scene (30 m resolution) acquired July 13, 2009 were used for all image texture analyses. From the Landsat satellite image we retained six spectral bands: Band 1 (Blue-green), Band 2 (Green), Band 3 (Red), Band 4 (Near-infrared), Band 5 (Mid-infrared), and Band 7 (Mid-infrared). Additionally, because numerous studies have shown a response by birds to vegetation biomass and greenness (Lee et al. 2004, Seto et al. 2004, Szép et al. 200), we calculated the Normalized Difference Vegetation Index, or NDVI, which characterizes biomass, using the following formula (Tucker 1979):

$$\frac{\text{Near-infrared (Band 4)} - \text{red (Band 3)}}{\text{Near-infrared (Band 4)} + \text{red (Band 3)}}$$

To summarize image texture, we used two approaches. The first was the plot approach, which is a simple summarization of raw digital number values from the infrared air photo values within the 100 m radius plot by mean or standard deviation. In the second approach we employed a moving window. Here, a texture measure is calculated within a window that constitutes a subset of the plot, and assigned to the central pixel. The window then shifts location by one pixel and the process is repeated. As in the plot approach, these numbers were then summarized by mean or standard deviation.

Since the scale (as represented by window size) of an image texture metric may affect the strength of its relationship with vegetation structure, several window sizes were examined. Image texture from the infrared air photo was calculated in 3x3, 7x7, 15x15, 21x21, 31x31, and 51x51 moving windows. Image texture from the six Landsat spectral bands and the NDVI was calculated in 3x3 windows, 5x5, 7x7, and 11x11 windows, the final size approximating the extent of the 100 m radius sample area surrounding each point. We did not use larger window sizes for the Landsat texture because large window sizes coupled with the 30 m pixel size would have incorporated land far outside the 100 m radius area covered by ground vegetation structure sampling. Texture measures were selected based on their demonstrated ability to characterize

vegetation (Kuplich et al. 2005, Lu and Batistella 2005, Tuominen and Pekkarinen 2005, Ge et al. 2006, Dobrowski et al. 2008). The first-order measures included variance, mean, and entropy. We calculated eight second-order texture measures (Table 1). The tool ‘zonal statistics’ in ArcGIS 9.1 was used to summarize the mean and standard deviation of each texture measure within each 100 m radius sample point area.

Table 1.: Eight second-order measures of image texture, calculated from a gray-level co-occurrence matrix (GLCM) ordered by texture group, with description of what they measure, and the statistic formula. Measures in bold were retained for comparison with field-measured vegetation structure characteristics.

| Texture Group | Second-order statistic | Statistic Description of Behavior | Statistic Formula[†] |
|------------------------------|-------------------------------|--|---|
| Contrast Group | Contrast | A measure of the amount of local variation in tone values among neighboring pixels. It is the opposite of homogeneity. | $\sum_{n=0}^{N-1} n^2 \left\{ \sum_{i=1}^N \sum_{j=1}^N p(i, j) \right\}_{ i-j =n}$ |
| | Dissimilarity | Similar to contrast and inversely related to homogeneity. | $\sum_{n=0}^{N-1} n \left\{ \sum_{i=1}^N \sum_{j=1}^N p(i, j) \right\}$ |
| | Homogeneity | A measure of homogenous tone values across an image. | $\sum_i \sum_j \frac{1}{1 + (i - j)^2} p(i, j)$ |
| Descriptive Statistics Group | Correlation | Linear dependency of tone values on those of neighboring pixels. | $\frac{\sum_i \sum_j (ij) p(i, j) - \mu_x \mu_y}{\sigma_x \sigma_y}$ |
| | Mean | Gray level average in the GLCM window. | $\sum_{i, j=0}^{N-1} p(i, j)$ |
| | Variance | Gray level variance in the GLCM window. | $\sum_{i, j=0}^{N-1} p_{i, j} (i - \mu_i)^2$ |
| | | | |

Table 1: continued

| Texture Group | Second-order statistic | Statistic Description of Behavior | Statistic Formula[†] |
|----------------------|-------------------------------|--|--|
| Orderliness Group | Angular Second Moment | High when the GLCM is locally homogenous. Similar to Homogeneity. | $\sum_i \sum_j \{f(i, j)\}^2$ |
| | Entropy | Shannon-diversity entropy. High when the tone values of the GLCM have varying values. Opposite of angular second moment. | $-\sum_i \sum_j p(i, j) \log(p(i, j))$ |

[†]From Haralick et al. (1973)

Since many first- and second-order statistics, calculated in several window sizes, were generated from each image, we first investigated the correlation among scales of each texture measure, and the correlation between different texture measures. Spearman rank correlation was used as a data reduction method to reduce the pool of texture metrics considered to only those with the highest probability of characterizing ground-measured vegetation structure. We eliminated from further consideration one of each pair of texture measures that were strongly correlated. As a rule, we retained the smallest window size for all remaining analysis. The smaller window sizes capture heterogeneity of tone values over small extents and since vegetation structure can change rapidly in this study system, we felt the smaller window size best matched the scale of our vegetation sampling

One-way analysis of variance (ANOVA), with habitat type as the treatment, was used to test for differences in the means of the indices of vegetation structure and texture, from both the infrared-air photo and the Landsat data. Significant ANOVAs were followed by using Tukey's adjustment for multiple comparisons. Levene's test was used to assess the equality of variance.

We used linear regression models to determine the amount of variance in ground measured vegetation structure that was associated with image texture metrics among and within habitats. If assumptions of constant variance (i.e., homoscedasticity) could not be met, models were excluded from analysis. If assumptions of linear relationships were not met, second-order polynomial (i.e., quadratic term) linear regression models were fit. We used an information theoretic criterion (AIC_c) to rank models (Burnham and Anderson 2002).

The role of remotely sensed data in accounting for avian patterns at Fort Bliss and Fort McCoy

Landscape indices have been shown to account for variation in avian patterns, particularly in ecosystems where patches have clearly defined edges (e.g. forests, agriculture) and so we conducted a thorough analysis of their usefulness in explaining variation in patterns of bird species at Fort Bliss. We did not conduct a parallel analysis involving landscape indices at Fort McCoy because the results from Fort Bliss suggested these indices had very poor explanatory power in the broad ecotones of the Chihuahuan Desert (Appendix A(1)). Fort McCoy in Wisconsin has similar gradual change in proportion cover among habitats.

For the avian community at both installations, we assessed the relationship between bird species richness and image texture, as well as the relationship between individual bird species abundance and image texture. Below we detail the methods at Fort Bliss first, and at Fort McCoy second.

At Fort Bliss we calculated 14 first- and second-order texture measures in eight different window sizes on a set of digital orthophotos (resolution of ~1 m) acquired in 1996. For each of the 42 plots, we summarized mean and standard deviation of each texture value within multiple window sizes. The relationship between image texture and average bird species richness was assessed using linear regression models. We then used multiple regression models to predict species richness as a function of multiple texture measures. For the univariate linear models we conducted model selection using the information theoretic approach. For both the univariate and multiple regression models, we assessed how well the models performed using adjusted R^2 values.

We next conducted an analysis at Fort Bliss to evaluate the usefulness of measures of habitat structure and productivity derived from Landsat TM satellite imagery. In addition to using six Landsat bands individually, we used NDVI as the basis of first-order and second-order image texture measures. Image texture summarization for the six Landsat TM bands and NDVI was accomplished using both the plot approach (simple summarization by mean or standard deviation), and the moving window approach. We thereby assessed texture at two spatial scales. The smallest scale, 0.81 ha (the size of a 3x3 window), corresponds roughly to the home range size of several bird species found in the study area.

The process of calculating image texture at Fort McCoy followed that outlined in the section “Testing the relationship between foliage height diversity and image texture at Fort McCoy,” above

In the analysis of this data we used Bayesian model averaging (BMA) to evaluate the relative contribution of measures of habitat structure and plant productivity for determining bird species richness. We fitted four models for each Landsat band as well as for NDVI: 1) a combination of texture measures only (i.e. 14 texture measures) both at the plot (simple) and window levels ($struct_p$ and $struct_w$), and 2) a combination of measures of habitat structure and productivity (mean NDVI) at the plot and window levels ($struct_p_prod_p$ and $struct_w_prod_w$). We proceeded this way because we were first interested in comparing the predictive ability of texture alone, and then we wanted to compare the relative contribution of habitat structure and plant productivity for predicting patterns of species richness. We included quadratic terms for the variables for which including a quadratic term significantly improved univariate linear models. We conducted the Bayesian model averaging analysis using the R package BMA (R Development Core Team 2005). We modified the BMA procedure to consider only models containing up to five predictor variables to prevent overfitting the data. Bayesian information criterion (BIC) values are used to calculate approximate posterior model probabilities for each fitted model (M_i) using the following formula:

$$\Pr(M_i | Data) \approx \frac{\exp(-BIC_i / 2)\pi_i}{\sum_j \exp(-BIC_j / 2)\pi_j}$$

where π_i is the prior probability for each model (Link and Barker 2006). We chose uniform prior probabilities ($1/R$; where R is the total number of models fitted) because we had no *a priori* reason to favor one model over another. Using a method proposed by Madigan and Raftery (1994), a set of parsimonious, data-supported models, is defined using the Occam’s window

approach with C=20. This set of models is then used for calculating averaged coefficient estimates with their respective standard deviations, and posterior probabilities for each variable (i.e. the probability that a coefficient is different from zero). We used these posterior probabilities as an indication of the relative contribution of each explanatory variable among the set of input variables in the model for explaining bird species richness. To compare the results with traditional classification-based approaches, we also fitted BMA models using the three landscape indices (number of habitat types, edge density, and proportion of dense habitat) calculated within each plot. We did not include proportion of sparse habitat because it was directly related to the proportion of dense habitat.

To evaluate predictive ability we used a leave-one-out cross-validation (LOOCV) approach to evaluate the predictive ability of the set of best fitting models (i.e. those selected based on the Occam's window criteria of C=20). The LOOCV approach was chosen rather than a k-fold approach because of the low number of observations (n=42). We predicted the value of the i^{th} observation using the regression coefficients obtained by fitting the model leaving the i^{th} observation out (So and Karplus 1997). We compared the predictive ability of each fitted model using the standard error of cross-validation prediction calculated as follows:

$$\sigma PRESS = \sqrt{\frac{\sum_{i=1}^N (y_i - \hat{y}_i)^2}{N - n - 1}}$$

where y_i is the value of the i^{th} observation, \hat{y}_i it the predicted value of the i^{th} observation using the reduced model, N = the number of observations (here N = 42), n = the number of predictors in the model (n = 1, 2, 3, 4, or 5 in our case). The numerator in this equation corresponds to the PRESS (Predicted Residuals Sums of Squares) statistic (Allen 1974). Here, we chose σ PRESS for comparing models rather than raw PRESS values because doing so allows comparing models with different numbers of variables. Small σ PRESS values indicate strong predictive ability. For comparison purposes, we calculated the adjusted coefficient of determination ($R^2_{\text{adj.}}$) and the BIC for the best predictive models used in the models averaging.

Fort McCoy analyses followed the procedures out lined for Fort Bliss analysis. Habitat models were first built of bird species richness. We conducted a thorough analysis of the relationship between image texture measures and bird species, and after inspection of these results, we limited further model development to eight measures of image texture (plot level texture, 2nd order contrast, entropy, and variance, all summarized by both mean and standard deviation. We analyzed the power of image texture calculated from both infrared aerial photograph data and from NDVI (based on the satellite image), as well as ground measured estimates of vegetation structure to account of patterns of avian species richness. We subsequently developed univariate models of abundance from all three sets of predictive data (air photos, satellite imagery, and ground-based data).

Finally, we developed broad-scale maps of abundance for a suite of species at each installation. Habitat models were built to explain abundance and occurrence of thirteen bird species on Fort Bliss, using the three years of avian point count data collected from 1996 to 1998. We summarized two types of variables to characterize components of bird habitat at the 42 study plots surveyed in the 1996-1998 breeding seasons (i.e., the plots used to build the statistical models): habitat heterogeneity and elevation. To characterize habitat heterogeneity, we quantified image texture in a 9x9 pixel window around each of the 12 point count stations within a given study plot. We chose a 9x9 window because, with 30 m resolution pixels, the resulting 270 m² square window approximates the spatial coverage of one 150-m radius point count.

We measured elevation from a 10-m resolution digital elevation model, and calculated the mean and coefficient of variation in elevation within a 27x27 pixel window around each point count station to approximate the spatial coverage of the point count and the image texture window. We calculated coefficient of variation in elevation to obtain a measure of ruggedness. We averaged the mean and coefficient of variation values obtained at a given plot across the 12 points to obtain plot-level measures of elevation.

Models included five measures of image texture and elevation variables. We used coefficient estimates obtained from Bayesian Model Averaging to build predictive maps of abundance and probability of occurrence across the study area. Maps were validated using point count data obtained from 42 independent study plots from 2006 to 2008. For each map, we overlaid the point count locations from the second field campaign on the predictive maps of abundance and probability of occurrence created from (1) each year of data separately (1996, 1997, and 1998) and from (2) a 3-yr average of the predictions. We then extracted the predicted values of abundance and probability of occurrence at each point count from these maps for the common and less common species respectively. We then averaged values of the 12 points for each plot to obtain plot-level measures of abundance and probability of occurrence for each model year and for the 3-yr average. We excluded from the validation set plots that contained missing data (i.e., points that were on pixels where the value of any of the habitat variables was outside the range of values of the original data used for building the models). This resulted in a set of 38 plots for validating the models. We evaluated the predictive abilities of the abundance models using the Mean Squared Error (MSE) between the predicted and the actual values on the square-root scale as noted above. Low MSE indicates good predictive ability. We calculated the area under the relative operating characteristic curves (AUC) to evaluate the predictive ability of the logistic models (Pearce and Ferrier 2000). AUC values between 0.7 and 0.9 suggest that the model discriminates presence-absence reasonably well, while values above 0.9 indicate very good discrimination.

For Fort McCoy, we followed the methods outlined above to develop installation-wide maps of abundance for three species; Grasshopper Sparrow, Eastern Bluebird, and Ovenbird. Development of additional maps and validation of maps using cross-validation is ongoing. Univariate models were developed using a set of four candidate texture measures, as well as ground based measures. Maps of predicted abundance of bird species were developed from the best image texture model for the species (elevation varies little across Fort McCoy, and thus was not included in models.)

Analysis of the impact of phenological variation on texture measures.

Based on our work at both installations, and other recent studies (e.g., Estes et al, 2008), measures of texture are well suited to quantify vegetation structure, and they are useful in models of bird and other wildlife habitat use patterns. However, with increasing use of image texture it must be noted that analysis involving images of different areas or multitemporal images of the same area need to take into account factors that may affect texture measures. In particular, the effect of phenology could significantly affect multitemporal analyses. This is both a challenge and a useful fact; the potential upside of phenological variation is that texture differences among multitemporal images could contain important information. We were interested in finding the degree to which measures of image texture are robust to phenological change. In addition, we were interested in understanding how phenology-related variability in texture measures differs

across different biomes, window sizes, and spectral bands. We also compared the stability of measures between biomes.

Three North American study sites were chosen, representing contrasting biomes: a desert scrub region in New Mexico, a mix of deciduous and evergreen forests in Ontario, Canada, and an area of deciduous forest and agriculture in Virginia. These sites correspond to Landsat TM path 33 row 38, path 27 row 26, and path 16 row 33, respectively. The New Mexico site was centered near Las Cruces, New Mexico, and includes areas of New Mexico, Texas, and Chihuahua, Mexico, and was composed primarily of desert scrub. The Ontario study site covered mostly southwestern Ontario with a small area of northern Minnesota also included, and was covered primarily of forests and small lakes. The Virginia site included portions of western Maryland, eastern West Virginia, and Virginia. The West Virginia portion of the image was dominated by deciduous forests on slopes of the Appalachian Mountains, with some agriculture in the valleys. Agriculture dominated most of the Virginia portion of the image, with some mountainous deciduous forest, including nearly all of Shenandoah National Park. For each study site, a collection of Landsat images was assembled; one image was chosen as the reference and the others were georeferenced to that image. A suite of texture measures were calculated for each of the images. Within each study site, the calculated texture measures were compared among image dates on a pixel-by-pixel basis. For each study site, band, texture measure, and window size combination, the coefficient of variation of each pixel was calculated among the different image dates in order to assess the inter-date variability of the textures measures.

Results and Discussion

The relationship between foliage height diversity and image texture at Fort McCoy

Vegetation structure versus image texture-To compare and contrast the strength of relationship between vegetation structure and image texture both within and among habitat types, scatterplots were constructed of the highest Spearman rank coefficient between vegetation structure indices and measures of image texture (Figure 9). Relationships between vertical vegetation structure (foliage height diversity) and image texture were positive and linear within and among habitat types. The relationships were less clear for horizontal vegetation structure and foliage volume.

The airphoto- based metrics with the strongest ability to predict vertical vegetation structure were second order variance and contrast, both summarized by mean ($r^2 = 0.75$ and 0.79 , respectively, both with p value < 0.01). Analysis of the satellite imagery revealed that plot based Band 4 texture, summarized by the mean, was strongly related to foliage height diversity ($r^2 = 0.74$, p -value < 0.01) and plot level Band 4 and NDVI values, both summarized by the mean, were also strong predictor of foliage height diversity ($r^2 = 0.74$, and $r^2 = 0.71$, respectively, with p -value < 0.01). These are relatively straightforward measures, and their use provides a way to characterize approximately three quarters of the variance in vertical vegetation structure.

In analyses of the ability of image texture to capture vertical vegetation structure *within* the three habitat types, we found that image texture was related to between 30 and 60 % of vertical structure variation. The standard deviation of NDVI entropy captured about 35% of variation in grassland structure. In savanna, approximately 30% of variation in ground measured vertical structure was characterized by airphoto-based mean of contrast and variance, and was not well characterized by satellite imagery. In woodland habitat, satellite image-based mean of Band 4 and mean NDVI were both related to 59% of variance in vertical structure.

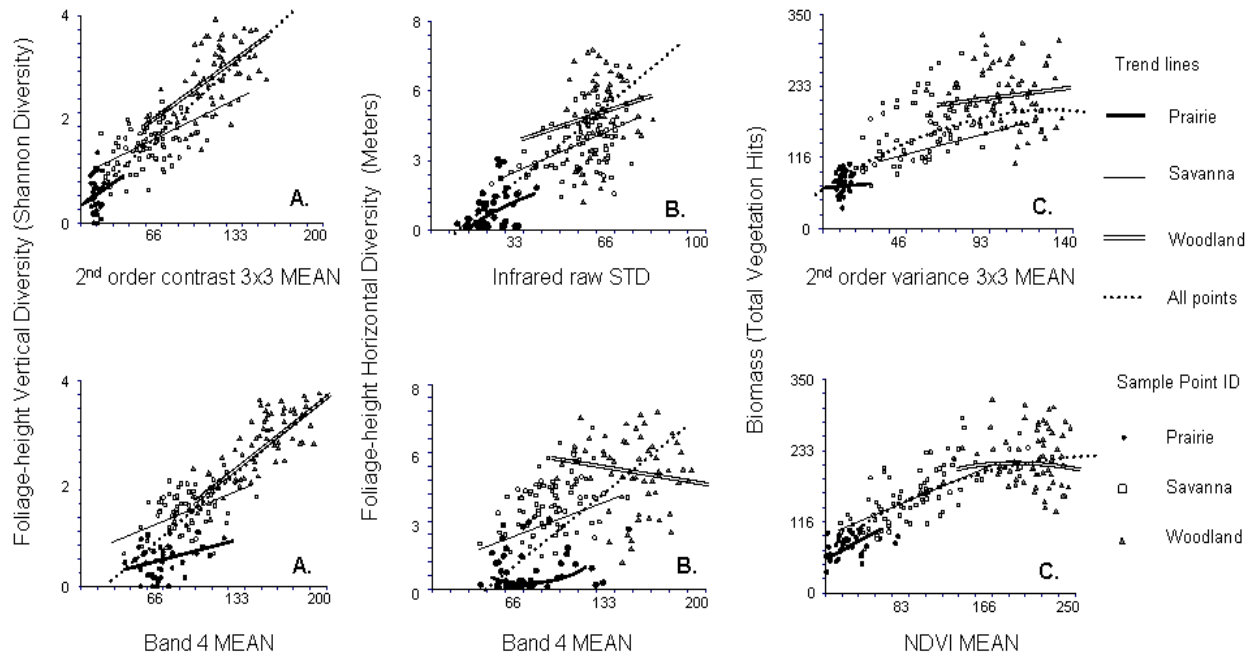


Figure 9. Scatterplots of vegetation structure variables vs. image texture values calculated from an infrared air photo (row 1) and Band 4 and NDVI from a Landsat scene (row 2); A) foliage height diversity, B) horizontal vegetation structure, represented by the variation of canopy heights measured in meters, and C) vegetation volume, measured as the total accumulation (or number of 'hits') of vegetation at a sample point. Correlations among habitats (i.e., all sample points among three habitat types) were assessed using Spearman-rank. The highest Spearman-rank correlation coefficient between texture measures and vegetation structure is plotted. To show within and among habitat relationships between vegetation structure, least-squares trend lines for linear relationships or second-order polynomial trend lines for quadratic relationships are plotted.

Bird Species richness models

At Fort Bliss, bird species richness varied greatly across habitats, with lowest species richness in grasslands, and highest richness in shrublands and pinyon-juniper. An average of 18 and 19 species occurred in black grama and mesa grasslands respectively. For the four shrublands, an average of 20 species occurred in sandsage, 23 in both creosote and mesquite, and 25 in whitethorn. Species richness was much higher in pinyon-juniper, with 34 species on average. Our analysis revealed that variation in bird species richness was strongly associated with image texture.

In the analysis of airphoto-derived image texture, we found that both 1st order and 2nd order texture measures had high predictive power. We also found that in general, there was no substantial gain in explanatory power when texture measures were calculated on edge-enhanced images over measures calculated on the unprocessed images. Single image texture measures derived from airphotos accounted for up to 57% of the variability in species richness (Table 2). Coupling elevation with a single texture measure (first order standard deviation, summarized by standard deviation) accounted for up to 63% of the variability in bird species richness. (St-Louis et al. 2006).

Table 2. Results from univariate linear regression models relating species richness to single image texture at different moving window sizes. Cell values represent the AICc w obtained for each individual window size for a given texture measure, for all models whose Δ AICc was smaller than 2. The AIC weight of the best moving window for a given texture is in bold. Corresponding values of AICc, adjusted R² and p-value are provided. The texture measures that best predicted species richness are underlined.

| Summary statistic | Measure type | Texture measure | Window size | | | | | | | | Best model AICc | Best model adjusted R ² | Best model p-value |
|-----------------------|-------------------------------------|-----------------|-------------|-------------|-------------|-------|-------------|-------------|-------------|-------------|-----------------|------------------------------------|--------------------|
| | | | 3x3 | 7x7 | 15x15 | 21x21 | 31x31 | 51x51 | 81x81 | 101x101 | | | |
| Standard deviation | 1 st order [†] | <u>SD</u> | | | | | 0.26 | 0.36 | 0.20 | | 238.34 | <u>56.67</u> | <0.001* |
| | | RG | | | 0.57 | | | | | | 256.56 | 33.14 | <0.001* |
| | | MIN | 0.42 | 0.19 | 0.36 | | | | | | 257.35 | 31.87 | <0.001* |
| | | MAX | 0.26 | 0.19 | | | 0.13 | 0.18 | | | 253.18 | 38.31 | <0.001* |
| | | <u>AVG</u> | | | 0.40 | | | | | | 245.50 | <u>48.62</u> | <0.001* |
| | 2 nd order ^{††} | ASM | 0.52 | | | | | | | | 269.75 | 8.46 | 0.035 |
| | | CON | 0.12 | 0.26 | 0.20 | 0.16 | 0.12 | | | | 263.34 | 21.43 | 0.001 |
| | | COR | | | 0.68 | 0.26 | | | | | 261.43 | 24.93 | <0.001 |
| | | DIS | | 0.21 | 0.33 | 0.23 | 0.13 | | | | 255.64 | 34.60 | 0.002 |
| | | ENT | | | | | | | 0.39 | 0.51 | 264.45 | 19.32 | <0.001 |
| | | <u>ICM1</u> | | | | | 0.75 | | | | 241.21 | <u>53.61</u> | <0.001* |
| | | <u>ICM2</u> | | | | 0.21 | 0.30 | 0.27 | | | 249.15 | <u>43.95</u> | <0.001* |
| | | IDM | | | | | | | | | ††† | | |
| | | <u>SSV</u> | | | | | | 0.32 | 0.40 | 0.23 | 240.73 | <u>54.13</u> | <0.001* |
| Mean of texture value | 1 st order | SD | | | | | | 0.15 | 0.27 | 0.36 | 260.61 | 26.37 | <0.001* |
| | | RG | | | | 0.10 | 0.12 | 0.16 | 0.22 | 0.26 | 264.01 | 20.17 | <0.001 |
| | | MIN | | | 0.11 | 0.14 | 0.17 | 0.18 | 0.18 | 0.18 | 264.43 | 19.36 | <0.001 |
| | | MAX | | | 0.66 | | | | | | 265.47 | 17.33 | 0.004 |
| | | AVG | | | | | | | | | | | |
| | 2 nd order | ASM | | | | 0.10 | 0.12 | 0.16 | 0.26 | 0.27 | 264.90 | 18.44 | 0.003 |
| | | CON | 0.13 | 0.13 | 0.13 | 0.12 | 0.13 | 0.12 | 0.12 | 0.13 | 270.22 | 7.44 | 0.044 |
| | | COR | | | | | | | 0.28 | 0.46 | 259.44 | 28.40 | <0.001 |
| | | DIS | 0.13 | 0.13 | 0.13 | 0.12 | 0.13 | 0.12 | 0.12 | 0.13 | 269.51 | 8.99 | 0.030 |
| | | ENT | | | | | | | 0.28 | 0.38 | 262.25 | 23.44 | <0.001 |
| | | ICM1 | | | | | | | | 0.66 | 254.80 | 35.88 | <0.001* |
| | | ICM2 | | | | | | | | | | | |
| | | IDM | 0.13 | 0.12 | 0.13 | 0.12 | 0.13 | 0.12 | 0.13 | 0.12 | 269.77 | 8.43 | 0.035 |
| | | SSV | | | | | | | 0.27 | 0.43 | 261.88 | 24.10 | <0.001 |

[†]First-order texture measures: SD = standard deviation, RG = range, MIN = minimum, MAX = maximum, AVG = average

^{††}Second-order texture measures: ASM = angular second moment, CON = contrast, COR = correlation, DIS = dissimilarity, ENT = entropy, ICM1 = information measure of correlation 1, ICM2 = information measure of correlation 2, IDM = inverse difference moment, SSV = sum of squares variance

^{†††} AICc is not shown for the models that were not significant from the linear regression analysis.

* Indicates cases where the model was still significant after Bonferonni correction (i.e., $p < 0.00224$)

Table 3. Range of R^2_{adj} , BIC, and σ PRESS values for the Fort Bliss species richness models used to obtain posterior probabilities using the Bayesian Model Averaging (BMA) approach. The table presents the results of models containing only measures of habitat structure at the plot ($struct_p$) and window ($struct_w$) levels, and measures of habitat structure and productivity at the plot ($struct_p + prod_p$) and window ($struct_w + prod_w$) levels. The number of models (Nb. Mod) that were used in the model averaging based on the Occam's window criteria of 20 is also indicated.

| Band | Model | Nb. Mod. | R^2_{adj} | BIC | σ PRESS |
|----------|---------------------|----------|-------------|---------|----------------|
| Blue | $struct_p$ | 31 | 45.4-58 | 249-254 | 4.7-5.8 |
| | $struct_w$ | 13 | 78.8-81.4 | 214-220 | 2.9-3.1 |
| | $struct_p + prod_p$ | 22 | 74.3-79.1 | 222-227 | 3.1-3.5 |
| | $struct_w + prod_w$ | 11 | 80.9-83 | 213-218 | 2.9-3.3 |
| Green | $struct_p$ | 33 | 45.9-54 | 250-255 | 4.6-5 |
| | $struct_w$ | 41 | 56.2-63.3 | 242-248 | 4.2-4.9 |
| | $struct_p + prod_p$ | 23 | 77.1-82.4 | 215-220 | 2.9-3.1 |
| | $struct_w + prod_w$ | 15 | 79.8-82.2 | 210-215 | 2.8-3 |
| Red | $struct_p$ | 22 | 53.4-56.7 | 244-250 | 4.2-4.5 |
| | $struct_w$ | 41 | 58.8-67.4 | 239-243 | 4-4.3 |
| | $struct_p + prod_p$ | 22 | 80.6-84.7 | 209-214 | 2.7-2.8 |
| | $struct_w + prod_w$ | 21 | 84.4-85.6 | 203-208 | 2.6-2.7 |
| NIR | $struct_p$ | 27 | 31.5-40.9 | 259-265 | 5-5.3 |
| | $struct_w$ | 40 | 38.1-46.4 | 256-262 | 4.8-5.1 |
| | $struct_p + prod_p$ | 23 | 80.3-84.6 | 209-214 | 2.7-2.9 |
| | $struct_w + prod_w$ | 11 | 84.5-84.9 | 203-207 | 2.6-2.7 |
| SWIR-TM5 | $struct_p$ | 42 | 60.3-72.3 | 233-238 | 3.5-4 |
| | $struct_w$ | 43 | 63-69.6 | 233-239 | 3.7-4 |
| | $struct_p + prod_p$ | 26 | 81.7-84.7 | 206-211 | 2.6-2.9 |
| | $struct_w + prod_w$ | 27 | 82-83.6 | 207-213 | 2.7-2.9 |
| SWIR-TM7 | $struct_p$ | 11 | 55.8-64.6 | 237-243 | 3.9-4.2 |
| | $struct_w$ | 33 | 60-72.4 | 233-239 | 3.6-4.1 |
| | $struct_p + prod_p$ | 26 | 83.3-86.1 | 202-207 | 2.5-2.7 |
| | $struct_w + prod_w$ | 26 | 81-84.1 | 207-212 | 2.7-2.8 |
| NDVI | $struct_p$ | 34 | 76.4-82.3 | 213-219 | 2.8-3.4 |
| | $struct_w$ | 22 | 75.8-80.9 | 217-223 | 3.1-3.4 |
| | $struct_p + prod_p$ | 22 | 85.5-87.4 | 196-201 | 2.4-3.2 |
| | $struct_w + prod_w$ | 26 | 82.4-86.3 | 204-209 | 2.6-2.8 |

In the satellite image based analysis, because we wanted to evaluate both the contribution of multiple measures of habitat structure and the relative importance of measures of habitat structure versus plant productivity for predicting species richness, we fitted models with texture alone (i.e., models $struct_p$ and $struct_w$), and models that included texture and mean NDVI as a proxy for plant productivity (i.e., models $struct_p + prod_p$ and $struct_w + prod_w$). Measures of habitat structure alone accounted for up to 81% (e.g., blue band) and up to 82% (from NDVI) of the variability in bird species richness (Table 3).

Models built with the 3x3 window-level data had lower σ PRESS values than those built using the plot-level data for all bands except for the SWIR-TM5 band. For NDVI, the results were very similar between the window and plot approach. These results suggest that models built using larger window sizes (e.g., 5x5 and 11x11) showed no substantial improvement over the smallest window size (3 x 3).

Models that incorporated both measures of habitat structure and plant productivity were better predictive models than models that were based only on habitat structure alone for all bands and for NDVI (Table 3). The models were very similar across all bands and for NDVI, both in terms of σ PRESS (as low as 2.4) and R^2_{adj} values, although measures derived from NDVI provided slightly better predictive models. Mean productivity (including its quadratic term) was chosen as a variable in all best fitting models, as shown by its posterior probability of 100% in all cases except for the blue band at the window level (Appendix A(2)). Combining up to five measures of habitat structure and productivity accounted for up to 87.4% of the variability in bird species richness (St-Louis et al. 2009).

A surprising result of this satellite imagery analysis was that the relationship between Near Infrared band (NIR) texture and bird species richness in the Chihuahuan Desert was quite weak. NIR is primarily sensitive to photosynthetically active vegetation, thus we were expecting a strong relationship between variability in vegetation greenness as captured by NIR and bird species richness. A possible explanation might be that, in this desert environment there is a very low contrast between soil and vegetation in the NIR wavelength (Franklin et al. 1993). Dry, bright soils can even induce NIR values that are greater than those of the vegetation present (Franklin et al. 1993). Because of the low contrast of the NIR band in this ecosystem the strong relationship between NDVI texture and bird species richness might depend more on the red band, which has lower reflectance values where there is high vegetation cover (Franklin et al. 1993). The mean red reflectance value is, in fact, very low for pinyon-juniper habitat in our study area, and higher for the grassland habitat. For the purpose of monitoring biodiversity, we can conclude from our results that NDVI is a suitable measure for capturing differences in productivity across habitats in this ecosystem.

At Fort McCoy, bird species richness ranged from as low as four species in grassland plots to as high as 36 species in savanna plots. The best models of species richness were derived from air photo data, and accounted for 52% of variability, while the best satellite image-based derived model, using the image texture measure NDVI contrast, accounted for 20% of variation (Figure 10). Not only was less variation in avian patterns explained in univariate models (57% at Fort McCoy vs 81% at Fort Bliss), but the strength of the two remotely sensed data products was reversed. Satellite image-based texture best characterized avian species richness in the Chihuahuan Desert, while air-photo-based texture performed best in the Wisconsin prairie-savanna-woodland ecosystem. We were surprised to find that at Fort McCoy where we explicitly tested the power of foliage height diversity and its derivatives to account for avian patterns, bird species richness was slightly better predicted by horizontal diversity (i.e., the standard deviation

of the height of vegetation at a plot), than by foliage height diversity *per se*, although image texture was the best predictor (Table 4).

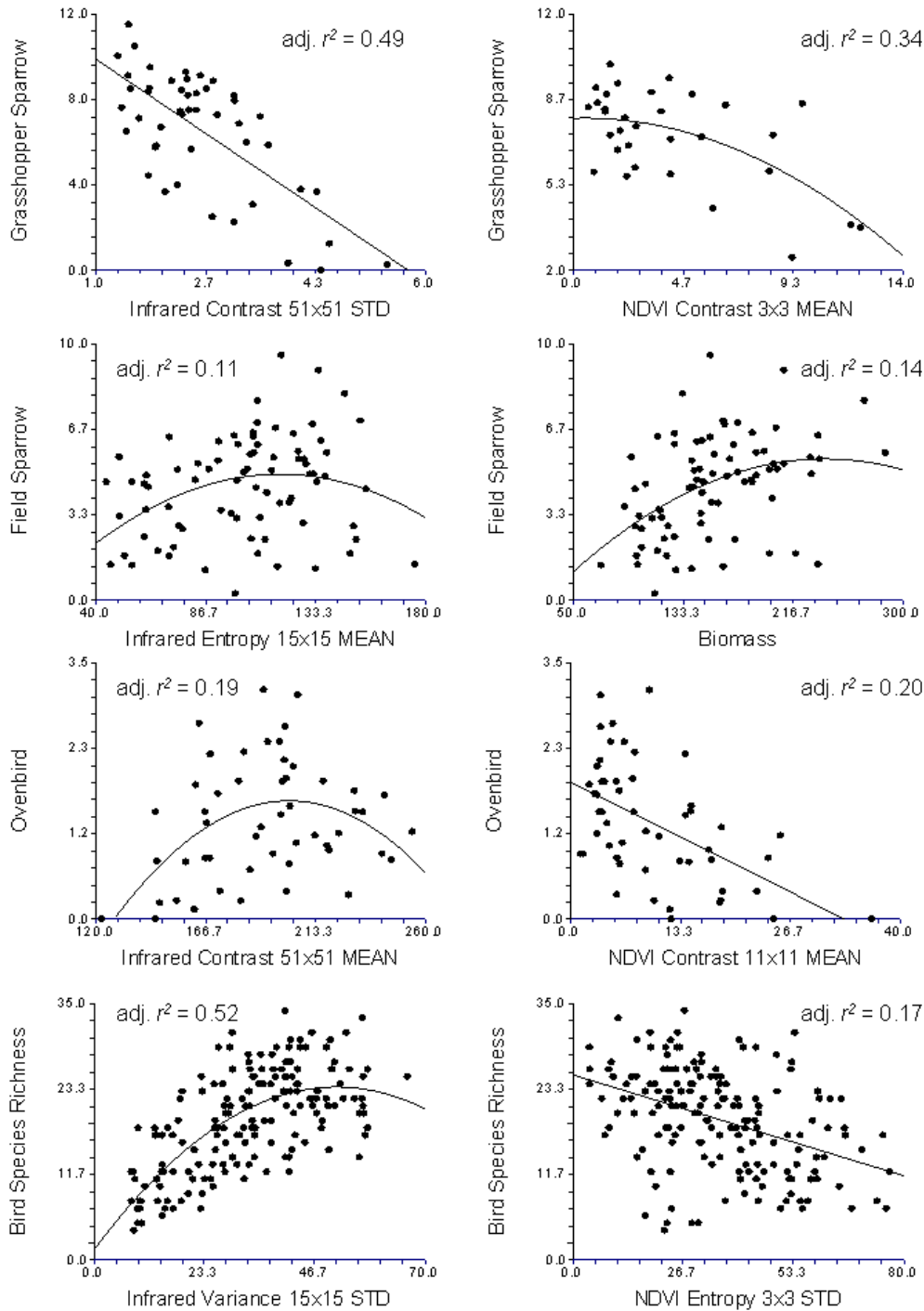


Figure 10. Scatterplots of predicted density of Grasshopper Sparrow at 32 grassland sample plots, Field Sparrow at 82 savanna plots, and Ovenbird at 52 woodland sample points, and bird species richness at 166 sample plots versus texture measures derived from infrared air-photo (left column), and NDVI (right column). A ground-collected vegetation metric, total vegetation volume, was superior to NDVI in predicting Field Sparrow density, therefore a scatterplot for this relationship is shown. The black lines represent results from linear regression with least-squares fitted and 2nd order polynomial lines.

Table 4. Fort McCoy species richness models. Fort McCoy results from univariate linear regression models relating species richness to image texture metrics at different window sizes. Three 2nd order texture measures, contrast, entropy, and variance were calculated on an infrared 1 meter resolution air photo or on 2) a vegetation index, NDVI from a Landsat TM scene and summarized by the mean and standard deviation in a 100 m radius circle surrounding sample points. The plot level texture is summarized by the mean and standard deviation, with no moving window analysis. Three ground based structural vegetation measures, vertical and horizontal diversity, and biomass are included to compare the amount of variance explained versus image texture metrics.

| Image Source | Summary Statistic | Texture Measure | Window Size | | | | | | Best model <i>p</i> -value |
|--|----------------------|-----------------|------------------|------|------|-------|-------|--------|----------------------------|
| | | | No Moving Window | 3x3 | 7x7 | 15x15 | 21x21 | 31x31 | |
| Infrared † | Mean | Plot | | | | | | | |
| | | Contrast | | | | | | | |
| | | Entropy | | | | | | | |
| | | Variance | | | | | | | |
| | Standard deviation | Plot | | | | | | | |
| | | Contrast | | | | | | | |
| | | Entropy | | | | 0.38 | | | |
| | | Variance | | 0.47 | | 0.52 | 0.50 | 0.46 | 0.37 |
| NDVI † | Mean | Plot | No Moving Window | 3x3 | 5x5 | 7x7 | 11x11 | | |
| | | Contrast | 0.12 | | | | | | <0.001 |
| | | Entropy | | | | | | | |
| | | Variance | | | | | | | |
| | Standard deviation | Plot | | | | | | | |
| | | Contrast | | | | | | | |
| | | Entropy | | 0.17 | 0.12 | 0.05 | | | <0.001 |
| | | Variance | | | | | | | |
| Ground Based Vegetation Measurements † | Vertical Diversity | | 0.32 | | | | | <0.001 | |
| | Horizontal Diversity | | 0.40 | | | | | <0.001 | |
| | Biomass | | | | | | | | |

† Columns that are not populated with model metrics indicate non-significance at the 5 % alpha level, or the assumptions of linear models could not be met

Species distribution models and maps of predicted probability of occurrence and abundance

Habitat models were built to explain abundance and occurrence of thirteen bird species on Fort Bliss, using the three years of avian point count data collected from 1996 to 1998. Predictive maps based on habitat models of abundance (Figure 11, Figure 12) and probability of occurrence (Figure 13, Figure 14) across the study area is shown. Validation of the predicted abundance models comparing mean square error of predicted and actual values showed generally small error values, suggesting overall very good predictive power.

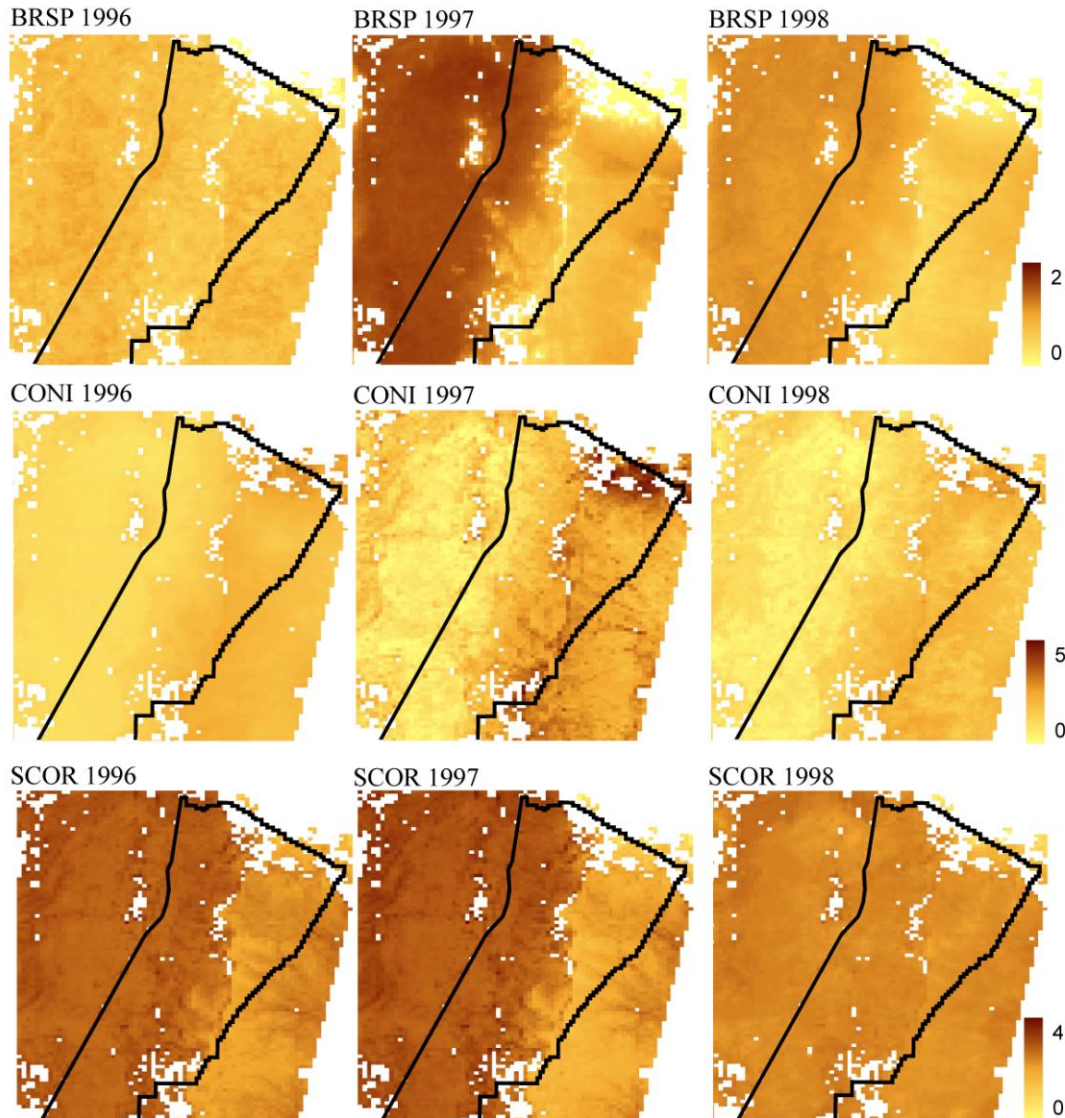


Figure 11. Predicted abundance of three species on McGregor Range of Fort Bliss. Pixels are 900 x 1200 m (108 ha). Darkest brown color indicates high abundance in each 108 ha plot (maximum is indicated by bar to the right of each row of maps), and lightest yellow indicates a predicted abundance of zero. Species acronym key: BRSP Brewer's Sparrow; CONI Common Nighthawk; SCOR Scott's Oriole.

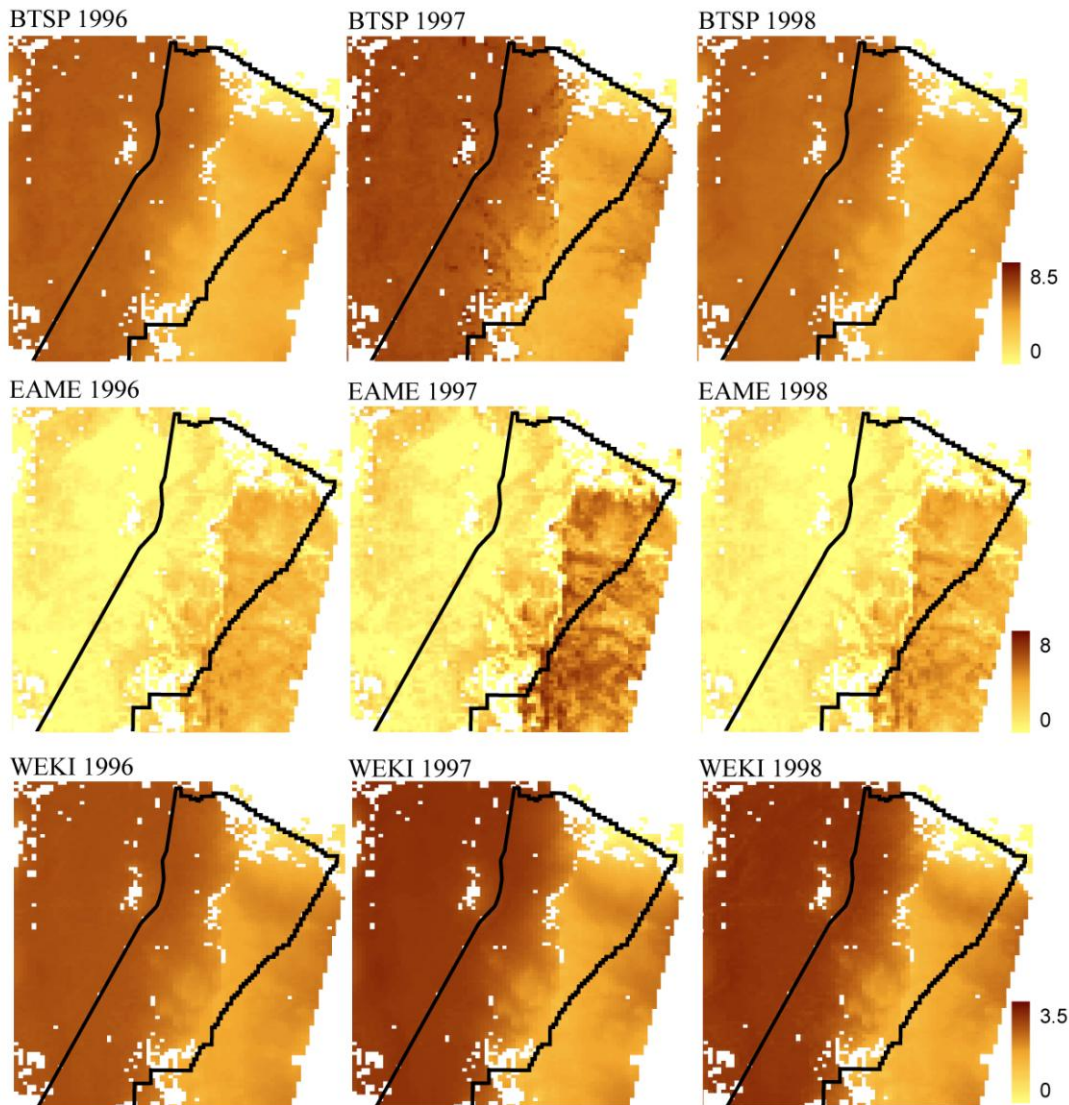


Figure 12. Predicted abundance of three additional species on McGregor Range of Fort Bliss. Pixels are 900 x 1200 m (108 ha). Darkest brown color indicates high abundance in each 108 ha plot (maximum is indicated by bar to the right of each row of maps), and lightest yellow indicates a predicted abundance of zero. Species acronym key: BTSP Black-throated Sparrow; EAME Eastern Meadowlark; WEKI Western Meadowlark.

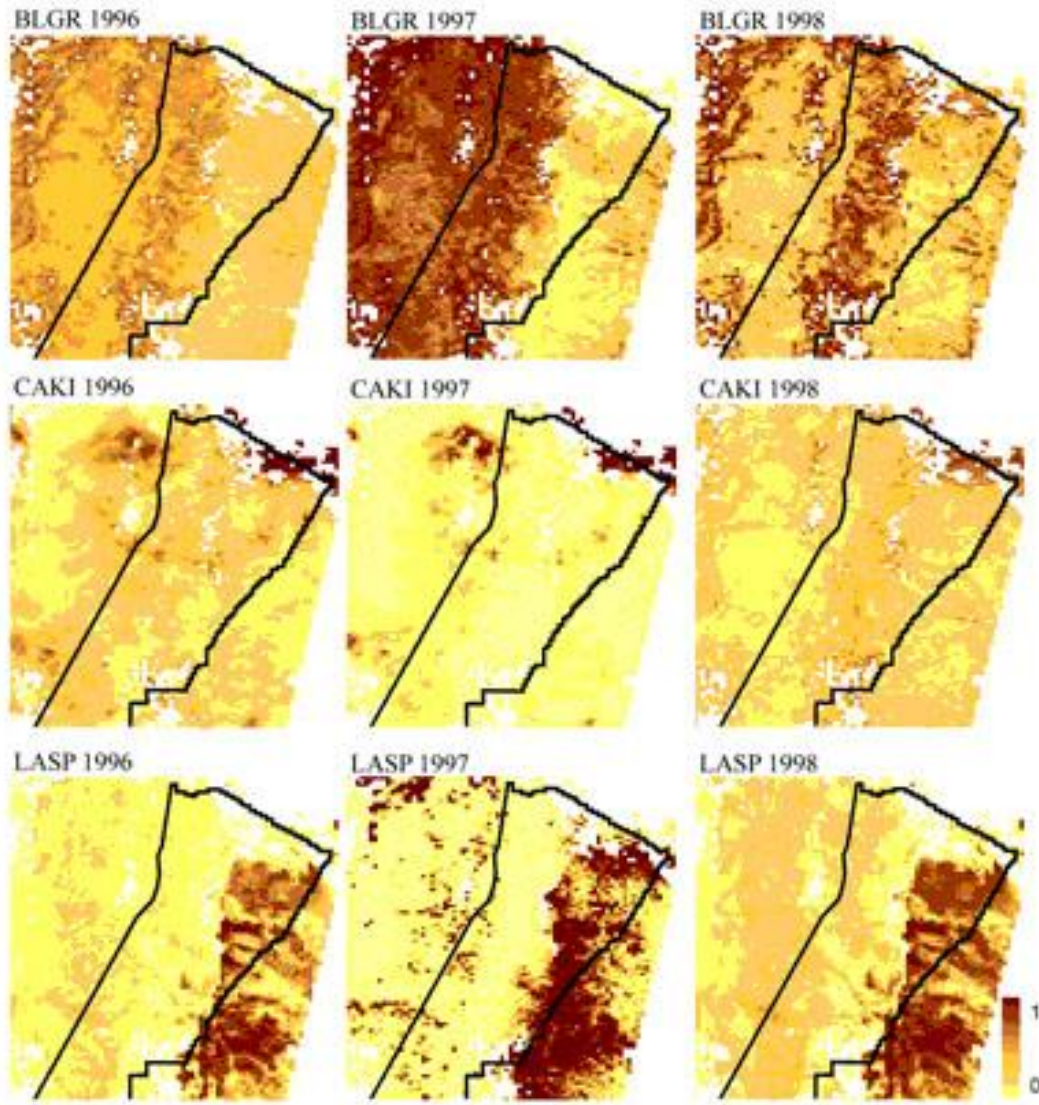


Figure 13. Predicted probability of occurrence of three bird species on McGregor Range, Fort Bliss. Pixels are 900 x 1200 m (108 ha). Darkest brown indicates highest probability of occurrence, while lightest yellow indicates no probability of occurrence. Species acronym key: BLGR Blue Grosbeak; CAKI Cassin's Kingbird; LASP Lark Sparrow.

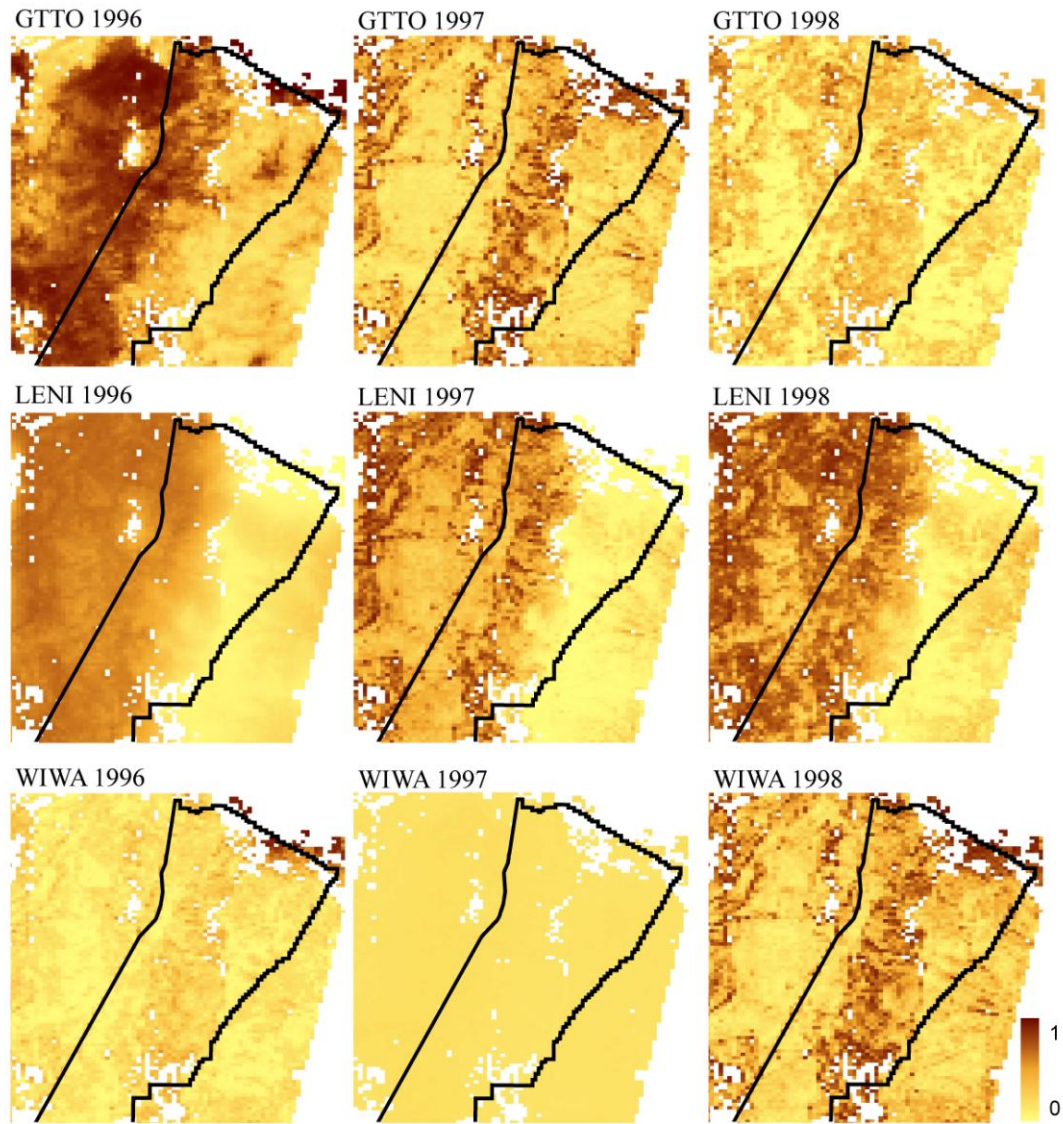


Figure 14. Predicted probability of occurrence of six more bird species on McGregor Range, Fort Bliss. Pixels are 900 x 1200 m (108 ha). Darkest brown indicates highest probability of occurrence, while lightest yellow indicates no probability of occurrence. Species acronym key: GTTO Green-tailed Towhee; LENI Lesser Nighthawk; WIWA Wilson's Warbler.

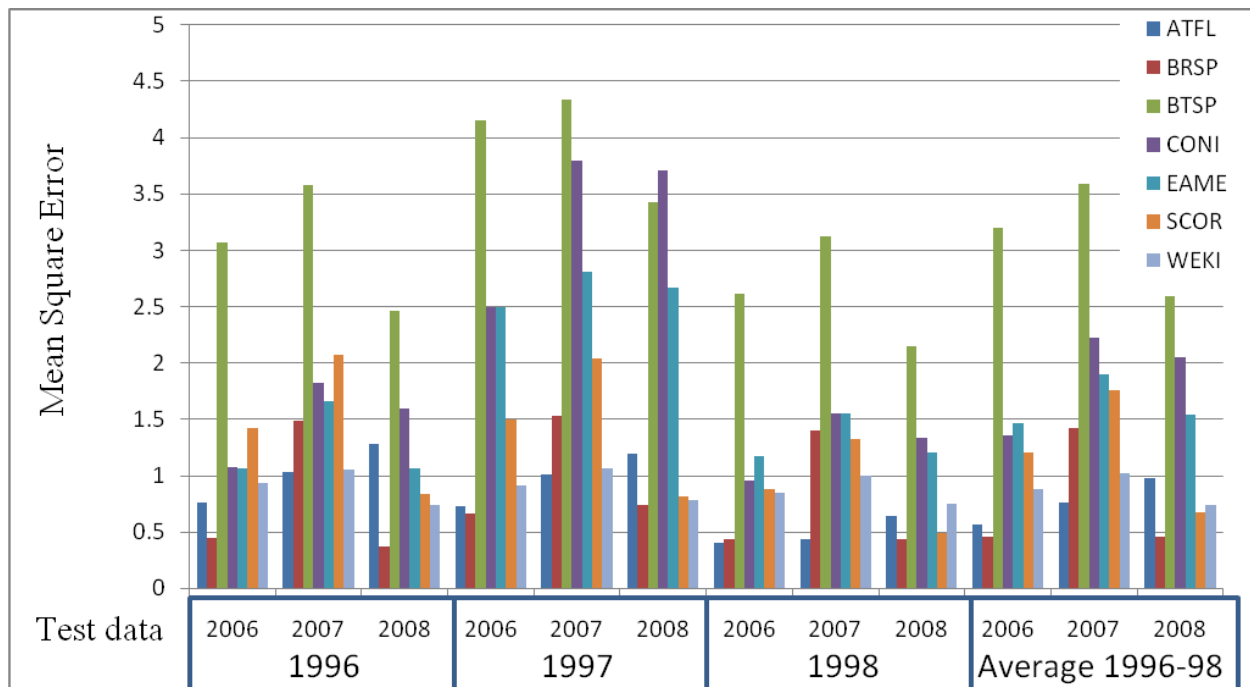


Figure 15. Maps of predicted species abundance were validated by comparing counts predicted at 42 new study plots (“test data” in figure, obtained in 2006 – 2008) against counts obtained in 1996-1998 at 42 original plots (“model data” in figure). The mean square error is the square of the difference between predicted and observed values. So, for example, a mean square error of 4 indicates a difference of approximately two individual birds per 108-ha plot. Key to four letter bird species codes are in list of acronyms.

Differences ranged from approximately one to two individuals per plot for the three year averages of Western Kingbird, and Scott’s Oriole, to approximately four birds per plot for Black-throated Sparrow, the most common species (Figure 15). The performance of models of bird species occurrence was less consistent. We obtained ‘good’ and ‘very good’ predictive power for some species in some years (e.g., Lark Sparrow, Lesser Nighthawk) but inconsistent predictive power among years for other species (e.g. Cassin’s Kingbird) and poor results for one species (Green-tailed Towhee) (Table 5). The three-year average of the predictions produced similar, if not higher performance as judged by the validation data, than models obtained from individual years.

The relative contribution of predictive variables for explaining the abundance and occurrence of birds varied across species and across years (Table 6). The contribution of specific measures of NDVI texture varied across species and years, although 1st order mean and coefficient of variation contributed to models more frequently than other measures. Mean and variability in elevation contributed highly to the models for Black-throated Sparrow, Eastern Meadowlark, Lark Sparrow, Lesser’s Nighthawk, Scott’s Oriole, and Western Kingbird.

Table 5. Validation of probability of occurrence maps, Fort Bliss. Area under the relative operating characteristic curve (AUC) values obtained to validate the probability of occurrence maps created using measures of texture and elevation for six species. The predicted probabilities of occurrence obtained using models built with the 1996, 1997, and 1998 data were validated using data collected in 2006, 2007, and 2008 respectively. A 3-yr average of the predictions was also calculated and validated using the same data. A prediction is considered “good” when the AUC is equal or larger than 0.70, and “very good” when the AUC is equal or larger than 0.90.

| Species | Model used to make predictions | Year of the validation data | AUC (Texture measures) | Predictive accuracy (Texture measures) |
|-------------------|--------------------------------|-----------------------------|------------------------|--|
| BLGR ^a | 1996 | 2006 | 0.72 | good |
| | | 2007 | 0.60 | |
| | | 2008 | 0.43 | |
| | 1997 | 2006 | 0.70 | |
| | | 2007 | 0.62 | |
| | | 2008 | 0.39 | |
| | 1998 | 2006 | 0.65 | |
| | | 2007 | 0.47 | |
| | | 2008 | 0.61 | |
| | Average of the three years | 2006 | 0.72 | good |
| | | 2007 | 0.59 | |
| | | 2008 | 0.46 | |
| CAKI | 1996 | 2006 | 0.76 | good |
| | | 2007 | 0.58 | |
| | | 2008 | 0.57 | |
| | 1997 | 2006 | 0.75 | good |
| | | 2007 | 0.58 | |
| | | 2008 | 0.57 | |
| | 1998 | 2006 | 0.81 | good |
| | | 2007 | 0.62 | |
| | | 2008 | 0.59 | |
| | Average of the three years | 2006 | 0.77 | good |
| | | 2007 | 0.55 | |
| | | 2008 | 0.58 | |
| GTTO | 1996 | 2006 | 0.61 | |
| | | 2007 | 0.63 | |
| | | 2008 | 0.50 | |
| | 1997 | 2006 | 0.64 | |
| | | 2007 | 0.53 | |
| | | 2008 | 0.68 | |
| | 1998 | 2006 | 0.49 | |
| | | 2007 | 0.47 | |
| | | 2008 | 0.70 | |
| | Average of the three years | 2006 | 0.57 | |
| | | 2007 | 0.56 | |
| | | 2008 | 0.62 | |

Table 5, continued

| Species | Model used to make predictions | Year of the validation data | AUC (Texture measures) | Predictive accuracy (Texture measures) | |
|---------|--------------------------------|-----------------------------|------------------------|--|-----------|
| LASP | 1996 | 2006 | 0.72 | good | |
| | | 2007 | 0.96 | very good | |
| | | 2008 | 0.94 | very good | |
| | 1997 | 2006 | 0.73 | good | |
| | | 2007 | 0.79 | good | |
| | | 2008 | 0.72 | good | |
| | 1998 | 2006 | 0.72 | good | |
| | | 2007 | 0.95 | very good | |
| | | 2008 | 0.95 | very good | |
| | Average of the three years | 2006 | 2006 | 0.85 | good |
| | | | 2007 | 0.93 | very good |
| | | | 2008 | 0.92 | very good |
| 1996 | | 2006 | 0.67 | good | |
| | | 2007 | 0.64 | | |
| | | 2008 | 0.57 | | |
| 1997 | 2006 | 0.73 | good | | |
| | 2007 | 0.64 | | | |
| | 2008 | 0.54 | | | |
| 1998 | 2006 | 2006 | 0.75 | good | |
| | | 2007 | 0.64 | | |
| | | 2008 | 0.56 | | |
| | Average of the three years | 2006 | 0.73 | good | |
| | | 2007 | 0.65 | | |
| | | 2008 | 0.56 | | |
| WIWA | 1996 | 2006 | 0.52 | | |
| | | 2007 | 0.49 | very good | |
| | | 2008 | 0.65 | | |
| | 1997 | 2006 | 0.63 | | |
| | | 2007 | 0.74 | | |
| | | 2008 | 0.17 | | |
| | 1998 | 2006 | 0.56 | | |
| | | 2007 | 0.46 | very good | |
| | | 2008 | 0.71 | good | |
| | Average of the three years | 2006 | 0.57 | | |
| | | 2007 | 0.50 | very good | |
| | | 2008 | 0.66 | | |

^a ATFL = Ash-throated Flycatcher, BLGR = Blue Grosbeak, BTSP = Black-throated Sparrow, BRSP = Brewer's Sparrow, CAKI = Cassin's Kingbird, CONI = Common Nighthawk, EAME = Eastern Meadowlark, GTTO = Green-tailed Towhee, LASP = Lark Sparrow, LENI = Lesser Nighthawk, SCOR = Scott's Oriole, WEKI = Western Kingbird, and WIWA = Wilson's Warbler.

Table 6. Mean density of birds at Fort McCoy. Mean density (\pm SE) per 0.3 ha plot, adjusted for detectability, as well as species richness and Shannon diversity, for vegetation types distributed along an open to closed canopy cover continuum. Species with same superscript (A-C) do not differ significantly in density between habitats (one-way ANOVA, $P > 0.05$).

| Species | | Sand Prairie | Oak Savanna | Oak Woodland |
|-------------------------------------|------------------------------------|------------------------------|------------------------------|------------------------------|
| Baltimore Oriole | (<i>Icterus galbula</i>) | 0.03 \pm 0.01 [†] | 1.21 \pm 0.21 ^A | 0.27 \pm 0.07 ^B |
| Brown-headed Cowbird | (<i>Molothrus ater</i>) | 0.19 \pm 0.09 ^A | 2.27 \pm 0.40 ^B | 1.14 \pm 0.15 ^C |
| Brown Thrasher ^{††*} | (<i>Toxostoma rufum</i>) | 0 \pm 0 | 0.45 \pm 0.09 | 0 \pm 0 |
| Clay-colored Sparrow ^{††*} | (<i>Spizella pallida</i>) | 0.16 \pm 0.03 ^A | 0.13 \pm 0.02 ^B | 0 \pm 0 |
| Chipping Sparrow | (<i>Spizella passerina</i>) | 0.25 \pm 0.09 ^A | 1.11 \pm 0.14 ^B | 0.21 \pm 0.04 ^A |
| Dickcissel ^{††*} | (<i>Spiza americana</i>) | 0.30 \pm 0.04 | 0.03 \pm 0.01 [†] | 0 \pm 0 |
| Eastern Bluebird | (<i>Sialia sialis</i>) | 0.16 \pm 0.03 ^A | 0.91 \pm 0.14 ^B | 0.02 \pm 0.01 [†] |
| Eastern Kingbird | (<i>Tyrannus tyrannus</i>) | 0.10 \pm 0.06 ^A | 0.50 \pm 0.07 ^B | 0 \pm 0 |
| Eastern Meadowlark ^{††*} | (<i>Sturnella magna</i>) | 0.28 \pm 0.03 [†] | 0.06 \pm 0.03 [†] | 0 \pm 0 |
| Eastern Towhee | (<i>Pipilo erythrophthalmus</i>) | 0.05 \pm 0.03 [†] | 0.82 \pm 0.06 ^A | 0.54 \pm 0.06 ^B |
| Eastern Wood-Pewee ^{††} | (<i>Contopus virens</i>) | 0 \pm 0 | 0.14 \pm 0.02 ^A | 0.47 \pm 0.03 ^B |
| Field Sparrow ^{††*} | (<i>Spizella pusilla</i>) | 0.51 \pm 0.14 ^A | 4.31 \pm 1.24 ^B | 0.45 \pm 0.13 ^A |
| Great-crested Flycatcher | (<i>Myiarchus crinitus</i>) | 0 \pm 0 | 0.08 \pm 0.03 ^A | 0.24 \pm 0.04 ^B |
| Gray Catbird | (<i>Dumetella carolinensis</i>) | 0.04 \pm 0.02 [†] | 0.88 \pm 0.29 | 0.02 \pm 0.01 [†] |
| Grasshopper Sparrow ^{††*} | (<i>Ammodramus Barrensrum</i>) | 6.34 \pm 1.18 ^A | 0.87 \pm 0.12 ^B | 0 \pm 0 |
| Horned Lark | (<i>Eremophila alpestris</i>) | 0.72 \pm 0.12 | 0 \pm 0 | 0 \pm 0 |
| House Wren | (<i>Troglodytes aedon</i>) | 0.04 \pm 0.03 [†] | 0.50 \pm 0.17 | 0.05 \pm 0.04 [†] |
| Indigo Bunting | (<i>Passerina cyanea</i>) | 0.09 \pm 0.10 [†] | 1.20 \pm 0.15 ^A | 0.81 \pm 0.16 ^B |

Table 6, continued

| Species | | Sand Prairie | Oak Savanna | Oak Woodland |
|--------------------------------------|---------------------------------------|---------------------------|---------------------------|---------------------------|
| Lark Sparrow [*] | (<i>Chondestes grammacus</i>) | 0.04 ± 0.05 [†] | 0.26 ± 0.10 | 0 ± 0 |
| Mourning Dove | (<i>Zenaida macroura</i>) | 0.22 ± 0.03 ^A | 0.41 ± 0.03 ^B | 0.05 ± 0.04 [†] |
| Orchard Oriole | (<i>Icterus spurius</i>) | 0 ± 0 | 0.44 ± 0.06 | 0 ± 0 |
| Ovenbird | (<i>Seiurus aurocapillus</i>) | 0 ± 0 | 0 ± 0 | 1.34 ± 0.16 |
| Rose-breasted Grosbeak ^{††} | (<i>Pheucticus ludovicianus</i>) | 0 ± 0 | 0.27 ± 0.04 ^A | 0.74 ± 0.16 ^B |
| Red-eyed Vireo | (<i>Vireo olivaceus</i>) | 0 ± 0 | 0.03 ± 0.04 [†] | 1.07 ± 0.19 |
| Red-headed Woodpecker ^{††*} | (<i>Melanerpes erythrocephalus</i>) | 0.01 ± 0.01 [†] | 0.08 ± 0.01 [†] | 0.02 ± 0.02 [†] |
| Scarlet Tanager | (<i>Piranga olivacea</i>) | 0 ± 0 | 0.10 ± 0.03 [†] | 0.50 ± 0.05 |
| Upland Sandpiper | (<i>Bartramia longicauda</i>) | 0.23 ± 0.03 | 0.03 ± 0.02 [†] | 0 ± 0 |
| Vesper Sparrow ^{††*} | (<i>Pooecetes gramineus</i>) | 1.16 ± 0.15 ^A | 1.52 ± 0.38 ^B | 0 ± 0 |
| Diversity | | | | |
| Species Richness | | 12.81 ± 0.76 ^A | 24.03 ± 0.56 ^B | 17.04 ± 0.71 ^C |
| Shannon Diversity | | 2.26 ± 0.05 ^A | 3.00 ± 0.04 ^B | 2.70 ± 0.05 ^C |

Notes: Superscript A-C: species with same superscript do not differ significantly between habitats (one-way ANOVA, P > 0.05).

[†] = Unadjusted density

^{††} = Partner's in Flight (PIF) Priority Species

^{*} = Species of Greatest Conservation Need (SGCN) for Wisconsin's Comprehensive Wildlife Conservation Plan (<http://www.wisconsinbirds.org/plan/species/priority.htm>)

For the Loggerhead Shrike, a species that is of conservation concern because it is declining over much of its range, we developed habitat models and assessed the degree to which adult abundance is an indicator of habitat quality, as determined by reproductive success. We also examined at which scale – local, intermediate, or broad- this species most strongly responds to habitat. We found that Shrike abundance is indeed an indicator of fitness, but that there was a clear absence of a relationship between habitat variables and nest-based measures of fitness. We also found that local-scale (those measured in the field, e.g., foliage height diversity and forb cover) and intermediate-scale (the image texture-based measure mean NDVI), but not broad-scale (e.g. landscape indices including proportion of grassland, and edge density) habitat variables explained Shrike occurrence (Table 7; St-Louis et al. 2010).

Table 7. Loggerhead Shrike on Fort Bliss: the spatial scales at which habitat was assessed, that best explained occurrence of adults and nests.

| | | Rank of Habitat Scale (Bayesian Information Criterion) |
|-----------------------------------|------------|---|
| Occurrence of Shrike adults | 1996 | Intermediate > Local > Broad 256 253 260 |
| | 1997 | Intermediate > Local > Broad 196 201 203 |
| | 1998 | Local > Intermediate > Broad 181 185 188 |
| Occurrence of shrike nests | 1996, 1997 | Intermediate = Broad |
| | 1998 | Intermediate |

Patterns of density of bird species at Fort McCoy reveal distinct patterns of habitat use. For example one set of birds clearly use savanna more than other species during the breeding seasons (e.g., Baltimore Oriole, Brown-headed Cowbird, Brown Thrasher, Eastern Bluebird, and Gray Catbird), whereas other species, represented by Grasshopper Sparrow, use grassland predominantly. Rose-breasted Grosbeak and Ovenbird are examples of species that use woodland primarily. Univariate models of species abundance at Fort McCoy were developed using a set of four texture measures, as well as ground based measures. We found that up to 50% of variation in Grasshopper Sparrow abundance was accounted for by airphoto-based image texture. Single variable models predicted field sparrow abundance poorly, and accounted for up to 20% of variation in Ovenbird abundance (Table 8). While image texture-based models did not account for >50% of variation in any of these species, models based on image texture did outperform or equal the explanatory power of models based on ground measured variables in every case. Maps derived from these models are shown for representative species of the three habitat structural classes (Figure 16).

Table 8. Fort McCoy models of abundance. Results from univariate linear regression models relating Grasshopper Sparrow, Field Sparrow, and Ovenbird density to image texture metrics at different window sizes (1x1 indicates no moving window). Three 2nd order texture measures, contrast, entropy, and variance were calculated on an infrared 1 meter resolution air photo or 2) a vegetation index, NDVI from a Landsat TM scene and summarized by the mean and standard deviation in a 100 m radius circle surrounding sample points. The simple texture is summarized by the mean and standard deviation, and not a moving window analysis. In addition, three ground based structural vegetation measurements, vertical and horizontal diversity, and biomass are included to compare the amount of variance explained versus image texture metrics.

| Grasshopper Sparrow | | | | | | | | | | | |
|--|--------------------------|------------------------|--------------------|------------|------------|--------------|--------------|--------------|--------------|---------------------------|--------|
| Image Source | Summary Statistic | Texture Measure | Window Size | | | | | | | Best model p-value | |
| | | | 1x1 | 3x3 | 7x7 | 15x15 | 21x21 | 31x31 | 51x51 | | |
| Infrared † | Mean | Plot | 0.26 | | | | | | | <0.001 | |
| | | Contrast | | 0.16 | 0.17 | 0.17 | 0.20 | 0.20 | 0.26 | <0.001 | |
| | | Entropy | | | | | | 0.11 | | 0.028 | |
| | | Variance | | | | | | | | | |
| | Standard deviation | Plot | | | | | | | | | |
| | | Contrast | | | 0.40 | 0.40 | 0.38 | 0.40 | 0.42 | 0.49 | <0.001 |
| | | Entropy | | | | | | | | 0.14 | 0.004 |
| | | Variance | | | 0.44 | 0.38 | 0.34 | 0.33 | 0.33 | 0.34 | <0.001 |
| NDVI † | Mean | Plot | 1x1 | 3x3 | 5x5 | 7x7 | 11x11 | | | | |
| | | Contrast | | | | 0.34 | 0.31 | | | 0.001 | |
| | | Entropy | | | | 0.19 | | | | 0.019 | |
| | | Variance | | | | | 0.33 | | | 0.002 | |
| | Standard deviation | Plot | | | | | | | | | |
| | | Contrast | | | | | | | | | |
| | | Entropy | | | | | | | | | |
| | | Variance | | | 0.14 | | | | | | 0.046 |
| Ground based vegetation measurement † | Vertical Diversity | | | | | | | | | | |
| | Horizontal Diversity | | | | | | | | | | |
| | Biomass | | | | | | | | | | |

Table 8, continued

| Field Sparrow | | | | | | | | | | |
|--|--------------------|----------------------|-------------|------|------|-------|-------|-------|----------------------------|-------|
| Image Source | Summary Statistic | Texture Measure | Window Size | | | | | | Best model <i>p</i> -value | |
| | | | 1x1 | 3x3 | 7x7 | 15x15 | 21x21 | 31x31 | | 51x51 |
| Infrared † | Mean | Plot | | | | | | | | |
| | | Contrast | | 0.09 | 0.09 | 0.09 | | 0.09 | 0.09 | 0.010 |
| | | Entropy | | | | | | | | |
| | | Variance | | 0.09 | 0.06 | | 0.05 | | 0.05 | 0.011 |
| | Standard deviation | Plot | | | | | | | | |
| | | Contrast | | | | | | | | |
| | | Entropy | | | | 0.14 | | | | 0.005 |
| | | Variance | | | | 0.04 | | | | 0.042 |
| NDVI † | Mean | Plot | | | | | | | | |
| | | Contrast | | | | | | | | |
| | | Entropy | | | | | | | | |
| | | Variance | | | | | | | | |
| | Standard deviation | Plot | | | | | | | | |
| | | Contrast | | | | | | | | |
| | | Entropy | | | | | | | | |
| | | Variance | | | | | | | | |
| Ground Based Vegetation Measurements † | | Vertical Diversity | | | | | | | | |
| | | Horizontal Diversity | | | | | | | | |
| | | Biomass | | 0.14 | | | | | <0.001 | |

† Columns that are not populated with model metrics indicate non-significance at the 5 % alpha level, or the assumptions of linear models could not be met.

Table 8, continued

| Ovenbird | | | | | | | | | | |
|--|--------------------|----------------------|-------------|------|------|-------|-------|-------|----------------------------|-------|
| Image Source | Summary Statistic | Texture Measure | Window Size | | | | | | Best model <i>p</i> -value | |
| Infrared † | Mean | Plot | 1x1 | 3x3 | 7x7 | 15x15 | 21x21 | 31x31 | 51x51 | |
| | | Contrast | | 0.17 | 0.18 | 0.18 | 0.18 | 0.18 | 0.19 | 0.002 |
| | | Entropy | | | | 0.17 | | | 0.07 | 0.003 |
| | | Variance | | | | | | | | |
| | Standard deviation | Plot | | | | | | | | |
| | | Contrast | | | 0.09 | | | | | 0.028 |
| | | Entropy | | | | | | | | |
| | | Variance | | | | | | | | |
| NDVI † | Mean | Plot | 1x1 | 3x3 | 5x5 | 7x7 | 11x11 | | | |
| | | Contrast | 0.14 | 0.16 | 0.19 | 0.14 | 0.15 | | 0.010 | |
| | | Entropy | | 0.06 | 0.11 | 0.11 | 0.17 | | 0.002 | |
| | | Variance | | | 0.18 | 0.12 | | | 0.001 | |
| | Standard deviation | Plot | | | | | | | | |
| | | Contrast | | | 0.14 | 0.10 | | 0.20 | | 0.002 |
| | | Entropy | | | | | | | | |
| | | Variance | | | | 0.15 | | | | 0.003 |
| Ground Based Vegetation Measurements † | | Vertical Diversity | | 0.10 | | | | | 0.009 | |
| | | Horizontal Diversity | | | | | | | | |
| | | Biomass | | | | | | | | |

† Columns that are not populated with model metrics indicate non-significance at the 5 % alpha level, or the assumptions of linear models could not be met.

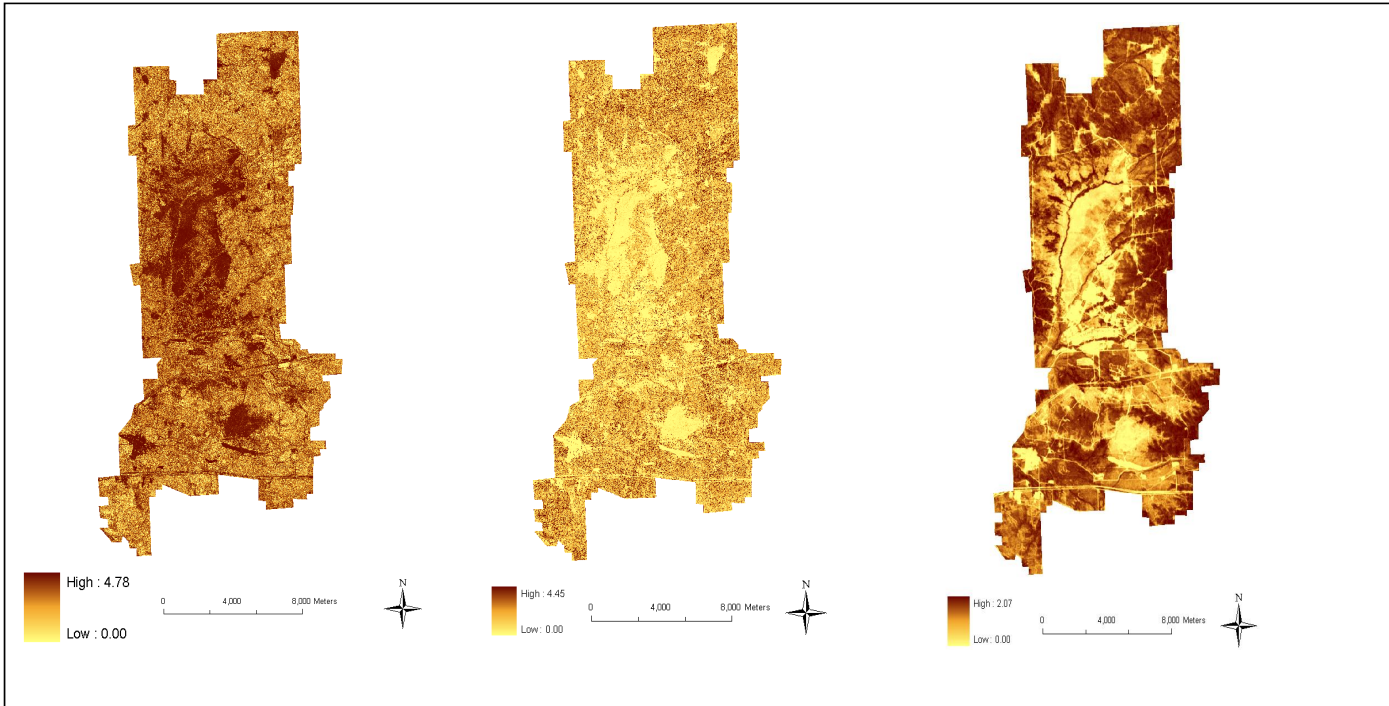


Figure 16. Maps of predicted average abundance of three species at Fort McCoy, WI. Grasshopper sparrow (left), Eastern bluebird (middle) and Ovenbird (right). Darkest brown color indicates high abundance in each 3.14 ha plot (maximum is indicated by bar to the left of each map), and lightest yellow indicates a predicted abundance of zero.

Our results suggest that measures that account for variability *within* landcover classes reflect fine-scale patterns of species abundance and occurrence that may not appear in maps based on models using landcover variables only, while retaining a broad-extent perspective. Habitat maps derived from classified satellite imagery are useful for generating patterns of species distribution at broad spatial extents but have limitations for addressing specific management or research questions when a finer spatial resolution is needed. The predictive maps of abundance and probability of occurrence that we derived reveal that abundance and occurrence of birds can be highly variable within land cover classes. These maps are thus useful in uncovering patterns of consistency and inconsistency in habitat use by a species.

The impact of phenological variation on texture measures.

In our study of three North American biomes, we found that inter-seasonal variability of texture measures was high overall indicating that care must be taken when using measures of texture at different phenological stages. This finding suggests that, to minimize the effect of phenological variation on texture measures, imagery used for comparisons should be selected for the same date or phenological stage. Special attention should be paid to land cover types, such as agriculture, that show high interseasonal or interannual variability. Certain texture measures, such as first-order mean and entropy (Figure 17) as well as second-order homogeneity, entropy, and dissimilarity (Figure 18), were more robust to phenological change than other measures. Interseasonal variability in texture measures was relatively unaffected by the window size chosen for the texture

calculations. This allows the flexibility to choose a window size based on a spatial scale(s) that is appropriate for a specific research question (Culbert et al. 2009).

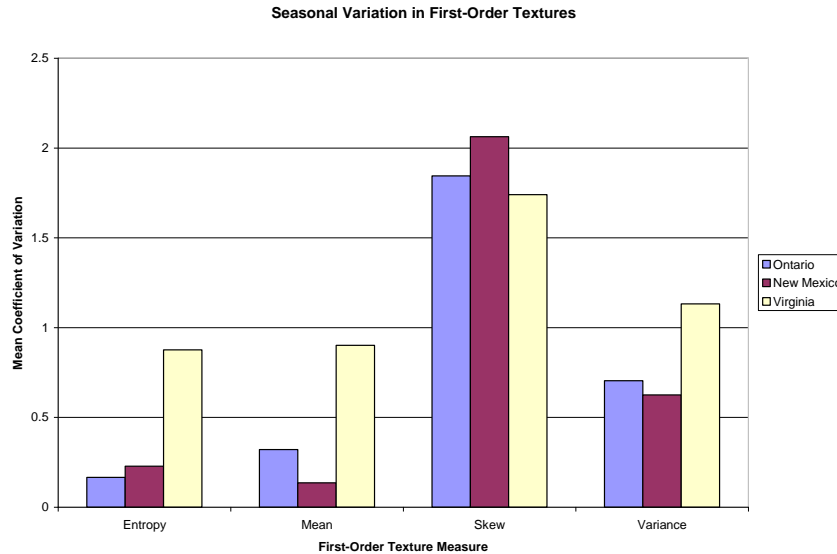


Figure 17 Mean image-wide coefficient of variation of first-order texture measures averaged across bands and three window sizes, for three study sites (New Mexico, Ontario, and Virginia). Entropy and mean had the lowest coefficient of variation. The Ontario and New Mexico study sites behaved similarly. Variation was generally higher in the Virginia site with a less distinct ranking of texture measure robustness.

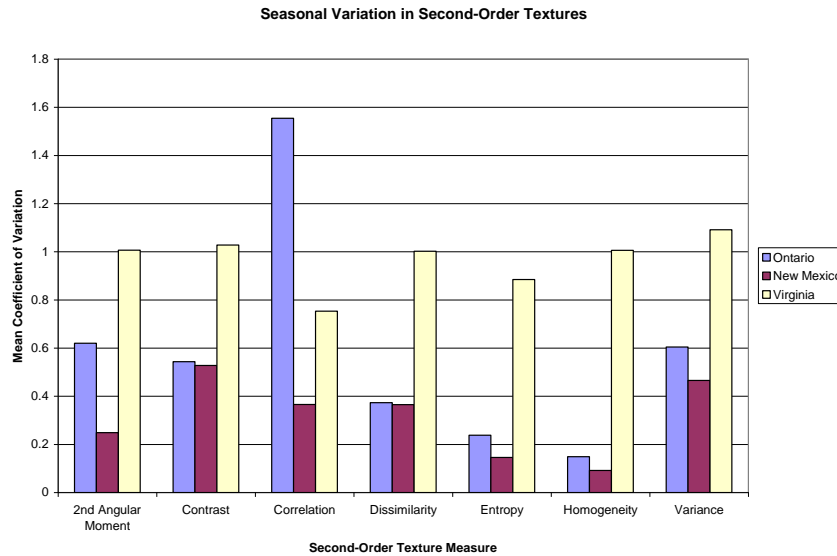


Figure 18. Mean image-wide coefficient of variation averaged across bands and three window sizes for each study site. Homogeneity and entropy were the most robust second-order measures. The Ontario and New Mexico sites behaved similarly. The Virginia site had higher variation and less distinction in robustness between different texture measures.

Conclusions and Implications for Future Research

It has long been known that vegetation structure is a key characteristic which influences habitat selection patterns of bird species. However, ornithologists and land managers have lacked adequate methods for measuring vegetation structure, as characterized by the foliage-height diversity method, across broad extents. This project has highlighted the potential to integrate remotely sensed measures of habitat structure in habitat models. We have identified strengths of this method, including the capability to characterize habitat structure at fine resolution and broad extent, the flexibility to summarize the digital numbers within remotely sensed data “as is”, or to calculate 1st or 2nd order image texture measures that are subsequently summarized. We also identified a particularly useful metric available from Landsat satellite imagery; image texture based on the Normalized Difference Vegetation Index. Band 4 (near-infrared) of Landsat imagery, is also strongly related to vegetation structure.

We found that habitat models based on image texture perform equal to or better than models based on classified habitat maps for characterizing habitat use across broad extents. Moreover, at Fort McCoy image texture based models performed better than the ground measured predictor foliage height diversity, the most commonly used field measurement in studies of avian habitat. There is a large array of image texture measures from which to choose. In the two open canopy ecosystems in which we worked, we did not find a particular set of texture measures that consistently and best characterized the variability in vegetation structure, species richness, and individual species abundance. This suggests that in each unique ecosystem, preliminary work will be required to understand the measures that perform best for a particular monitoring or management goal, whether it is to determine presence, distribution, or abundance of species of interest.

Natural disturbances, such as fires and hurricanes, are important in shaping habitat for many species. Image texture, by virtue of its ability to characterize fine details, has great potential for use in habitat models for species that apparently respond to subtle differences in cover, such as the variations in cover after fire. Future research into the usefulness of image texture for monitoring or characterizing post-disturbance habitat is an avenue worthy of further study.

Another avenue for future research could be to exploit phenological differences among air photos or satellite images, and to use texture measures from multiple seasons to improve habitat models. Similarly, thought must be given to the time of year in which remotely sensed data is best acquired for specific applications. For example, is imagery acquired during the season that data on the response variable is collected (in this study, breeding bird habitat use) in fact the best source of data for characterizing patterns? Might imagery from just prior to use period be better, because it reflects conditions when wildlife made habitat selection decisions?

However, while more work can be done, our study represents a major step forward for habitat assessments across large areas. For DoD natural resource biologists image texture is a source of information useful in estimating patterns of distribution of species and communities of interest, and will contribute to more thorough future INRMPs.

Literature Cited

- Asner, G.P., Wessman, C.A., Bateson, C.A., and Privette, J.L. 2000. Impact of tissue, canopy, and landscape factors on the hyperspectral reflectance variability of arid ecosystems. *Remote Sensing of Environment* **74**: 69-84.
- Aspinall R., N. Veitch. 1993. Habitat mapping from satellite imagery and wildlife survey data using a Bayesian modeling procedure in a GIS. *Photogrammetric Engineering and Remote Sensing* **59**:537-543.
- Bailey, R. G. 1995. Description of Ecoregions of the United States. Online version: <http://www.fs.fed.us/land/ecosysgmt/>
- Bergin T. M., L. B. Best, K. E. Freemark, and K. J. Koehler. 2000. Effects of landscape structure on nest predation in roadsides of midwestern agroecosystem: a multiscale analysis. *Landscape Ecology* **15**:131-143.
- Cody M. L. 1981. Habitat Selection in Birds - the Roles of Vegetation Structure, Competitors, and Productivity. *Bioscience* **31**:107-113.
- Coulter M. C., A. L. Bryan, H. E. Mackey, J. R. Jensen, and M. E. Hodgson. 1987. Mapping of Wood Stork Foraging Habitat with Satellite Data. *Colonial Waterbirds* **10**:178-180.
- Estades, C. F. (1997). Bird-habitat relationships in a vegetational gradient in the Andes of central Chile. *Condor* **99**:719-727.
- Estes L. D., G. S. Okin, A. G. Mwangi, and H. H. Shugart. 2008. Habitat selection by a rare forest antelope: A multi-scale approach combining field data and imagery from three sensors. *Remote Sensing of Environment* **112**:2033-2050.
- Flather C. H., J. R. Sauer. 1996. Using Landscape Ecology to Test Hypotheses About Large-Scale Abundance Patterns in Migratory Birds. *Ecology* **77**:28-35.
- Franklin J., D. W. Steadman. 1991. The Potential for Conservation of Polynesian Birds through Habitat Mapping and Species Translocation. *Conservation Biology* **5**:506-521.
- Franklin J., J. Duncan, and D. L. Turner. 1993. Reflectance of Vegetation and Soil in Chihuahuan Desert Plant-Communities from Ground Radiometry using Spot Wavebands. *Remote Sensing of Environment* **46**:291-304.
- Fretwell S. D., H. D. Lucas Jr. 1970. On territorial behavior and other factors influencing habitat distribution in birds; theoretical development. *Acta Biotheoretica* **19**:16-36.
- Fuller R. M., G. B. Groom, S. Mugisha, P. Ipulet, D. Pomeroy, A. Katende, R. Bailey, and R. Ogutu-Ohwayo. 1998. The integration of field survey and remote sensing for biodiversity assessment: a case study in the tropical forests and wetlands of Sango Bay, Uganda. *Biological Conservation* **86**:379-391.
- Gonnet J. M. 2001. Influence of Cattle Grazing on Population Density and Species Richness of Granivorous Birds (*Emberizidae*) in the and Plain of the Monte, Argentina. *Journal of Arid Environments* **48**:569-579.
- Griffiths G. H., J. Lee, and B. C. Eversham. 2000. Landscape pattern and species richness; regional scale analysis from remote sensing. *International Journal of Remote Sensing* **21**:2685-2704.
- Grinnell J. 1917. The niche-relationships of the California Thrasher. *Auk* **34**:427-433.
- Gutzwiller K. J., W. C. Barrow. 2002. Does Bird Community Structure Vary With Landscape Patchiness? A Chihuahuan Desert Perspective. *Oikos* **98**:284-298.

- Haralick R. M. 1979. Statistical and Structural Approaches to Texture. Proceedings of the IEEE **67**:786-804.
- Haralick R. M. 1973. Glossary and Index to Remotely Sensed Image Pattern-Recognition Concepts. Pattern Recognition **5**:391-403.
- Hepinstall J. A., S. A. Sader. 1997. Using Bayesian Statistics, Thematic Mapper Satellite Imagery, and Breeding Bird Survey Data to Model Bird Species Probability of Occurrence in Maine. Photogrammetric Engineering and Remote Sensing **63**:1231-1237.
- Herkert J. R. 1994. The effects of habitat fragmentation on midwestern grassland bird communities. Ecological Applications **4**:461-471.
- Hodgson M. E., J. R. Jensen, H. E. Mackey Jr, and M. C. Coulter. 1988. Monitoring wood stork foraging habitat using remote sensing and geographic information systems. Photogrammetric Engineering and Remote Sensing **55**:1601-1607.
- Imhoff M. L., T.D. Sisk, A. Milne, G. Morgan, and T. Orr. 1997. Remotely sensed indicators of habitat heterogeneity; use of synthetic aperture radar in mapping vegetation structure and bird habitat. Remote Sensing of Environment **60**:217-227.
- Karr, J. R., & R. R. Roth. (1971). Vegetation structure and avian diversity in several new world areas. *The American Naturalist* 105:423.
- Kozma J. M., N. E. Mathews. 1997. Breeding Bird Communities and Nest Plant Selection in Chihuahuan Desert Habitats in South-Central New Mexico. Wilson Bulletin **109**:424-436.
- Krueper D., J. Bart, and T. D. Rich. 2003. Response of Vegetation and Breeding Birds to the Removal of Cattle on the San Pedro River, Arizona (USA). Conservation Biology **17**:607-615.
- Laperriere A. J., P. C. Lent, W. C. Gassaway, and F. A. Nodler. 1980. Use of Landsat Data for Moose-Habitat Analyses in Alaska. Journal of Wildlife Management **44**:881-887.
- Lima S. L., and T. J. Valone. 1991. Predators and avian community organization: An experiment in a semi-desert grassland. Oecologia **86**:105-112.
- Luoto, M., Toivonen, T., and Heikkinen, R.K. 2002. Prediction of total and rare plant species richness in agricultural landscapes from satellite images and topographic data. Landscape Ecology 17: 195-217.
- MacArthur R. H. 1972. Geographical ecology: Patterns in the distribution of species. Harper and Row, New York.
- MacArthur R. H., R. Levins. 1964. Competition, habitat selection and character displacement in a patchy environment. Proceedings of the National Academy of Sciences **51**:1207-1210.
- MacArthur R. H., and J. W. MacArthur. 1961. On bird species diversity. Ecology **42**:594-598.
- Mills G. S., J. B. Dunning Jr., and J. M. Bates. 1991. The relationship between breeding bird density and vegetation volume. Wilson Bulletin **103**:468-479.
- Naranjo L. G., R. J. Raitt. 1993. Breeding Bird Distribution in Chihuahuan Desert Habitats. Southwestern Naturalist **38**:43-51.
- Patterson, M. P., & L. B. Best. (1996). Bird abundance and nesting success in Iowa CRP fields: The importance of vegetation structure and composition. *American Midland Naturalist* 135:153-167.

- Pidgeon A. M., V. C. Radeloff, and N. E. Mathews. 2003. Landscape scale patterns of Black-throated Sparrow (*Amphispiza bilineata*) abundance and nest success. *Ecological Applications* **13**:530-542.
- Pidgeon A. M., N. E. Mathews, R. Benoit, and E. V. Nordheim. 2001. Response of avian communities in the northern Chihuahuan Desert to historic habitat change. *Conservation Biology* **15**:1772-1788.
- Reeves H. M., F. G. Cooch, and R. E. Munro. 1976. Monitoring Arctic Habitat and Goose Production by Satellite Imagery. *Journal of Wildlife Management* **40**:532-541.
- Rosenzweig M. L. 1981. A theory of habitat selection. *Ecology* **62**:327-335.
- Rosenzweig, M. L. (1995). *Species diversity in space and time*. Cambridge University Press, Cambridge, UK.
- Rotenberry, J. T., & J. A. Wiens. (1980). Habitat structure, patchiness, and avian communities in north american steppe vegetation: A multivariate analysis. *Ecology* **61**:1228-1250.
- Saveraid E. H., D. M. Debinski, K. Kindscher, and M. E. Jakubauskas. 2001. A comparison of satellite data and landscape variables in predicting bird species occurrences in the Greater Yellowstone Ecosystem, USA. *Landscape Ecology* **16**:71-83.
- Stoms D. M., J. E. Estes. 1993. A Remote-Sensing Research Agenda for Mapping and Monitoring Biodiversity. *International Journal of Remote Sensing* **14**:1839-1860.
- Svardson G. 1949. Competition and habitat selection in birds. *Oikos* :157-174.
- Szaro R. C., M. D. Jakle. 1985. Avian use of a Desert Riparian Island and its Adjacent Scrub Habitat. *Condor* **87**:511-519.
- Tomoff C. S. 1974. Avian species diversity in desert scrub. *Ecology* **55**:396-403.
- Trzcinski M. K., L. Fahrig, and G. Merriam. 1999. Independent effects of forest cover and fragmentation the distribution of forest breeding birds. *Ecological Applications* **9**:586-593.
- Turner M. G. 1989. Landscape ecology: the effect of pattern on process. *Annual Review of Ecology and Systems* **20**:171-197.
- Wiens, J. A., & J. T. Rotenberry. (1981). Habitat associations and community structure of birds in shrubsteppe environments. *Ecological Monographs* **51**:21-42.

Appendix A – supporting material

Appendix A(1) . Adjusted R^2 from the relationship between average species richness and image landscape indices from Melhop's (1996) classification of habitats of McGregor Range of Fort Bliss Military Reserve, New Mexico.

| Landscape indices | Adjusted R^2 |
|--|----------------------------------|
| Classes present | 0.97 |
| Aggregation Index | 3.24 |
| Angular Second Moment | 10.47 |
| Avg. Polygon Perimeter-Area ratio (corrected) | -0.21 |
| Avg. Polygon Perimeter-Area ratio | 1.17 |
| Contagion | -0.94 |
| Dominance | 0.76 |
| Edge Density | 1.23 |
| Edge Distribution Evenness | 6.12 |
| Fractal Dimension (Box) | -1.91 |
| Fractal Dimension (Perimeter-Area) | -2.27 |
| Inverse Difference Moment | 7.95 |
| Largest Polygon Index | 8.76 |
| Perimeter | 2.73 |
| Total Polygons | 3.03 |
| Mean Polygon Area | 8.92 |
| Std. Dev. Polygon Area | 13.28 |
| Median Polygon Area | 2.66 |
| First Quartile Polygon Area | 2.14 |
| Third Quartile Polygon Area | -0.59 |
| Minimum Polygon Area | 4.84 |
| Maximum Polygon Area | 10.23 |
| Mean Polygon Perimeter | 7.37 |
| Std. Dev. Polygon Perimeter | 10.16 |

| | |
|----------------------------------|-------|
| Median Polygon Perimeter | 0.23 |
| First Quartile Polygon Perimeter | 0.91 |
| Third Quartile Polygon Perimeter | -0.36 |
| Minimum Polygon Perimeter | 4.84 |
| Maximum Polygon Perimeter | -0.15 |
| Relative Contagion | 6.11 |
| Relative Dominance | 5.25 |
| Shannon Weaver Diversity | 9.53 |
| Shannon Weaver Evenness | 5.34 |
| Mean Shape Index | 0.00 |
| Standard Deviation Shape Index | -0.86 |
| Median Shape Index | -2.43 |
| First Quartile Shape Index | 1.21 |
| Third Quartile Shape Index | -1.48 |
| Minimum Shape Index | 0.00 |
| Maximum Shape Index | -2.42 |

Appendix A(2). A measure of confidence in models of species richness at McGregor Range, Fort Bliss, developed from Landsat TM imagery. Numbers in cells indicate posterior probabilities of habitat structure and productivity (Prod.) measures resulting from the Bayesian Model Averaging approach for the models containing only texture measures at the plot ($struct_p$) and window ($struct_w$) levels, and texture measures and mean NDVI also at the plot ($struct_p + prod_p$) and window ($struct_w + prod_w$) levels. The superscript numbers in parenthesis indicate the posterior probabilities for the quadratic term, when it was included in the models.

| Band | Model | Habitat structure | | | | | | | | | | | | | | Prod. |
|-------|---------------------|-------------------|-------------------|--------------------|----------------------|-----|-----|-----|------|------|-----|-----|--------------------|------------------|--------------------|----------------------|
| | | asm | con | cor | cv | den | dva | ent | icm1 | icm2 | idm | mcc | rg | sen | sva | ndvi |
| Blue | $struct_p$ | 6 ⁽⁸⁾ | 11 ⁽⁸⁾ | 3 | 100 | 54 | 0 | 18 | 16 | 10 | 9 | 5 | 28 ⁽⁴³⁾ | 20 | 52 | NA* |
| | $struct_w$ | 5 ⁽⁰⁾ | 5 | 6 ⁽⁵⁾ | 100 ⁽¹⁰⁰⁾ | 95 | 100 | 6 | 12 | 8 | 9 | 7 | 0 | 0 ⁽⁵⁾ | 0 | NA |
| | $struct_p + prod_p$ | 8 ⁽²³⁾ | 1 ⁽⁰⁾ | 14 | 69 | 28 | 0 | 12 | 46 | 22 | 10 | 1 | 1 ⁽¹⁾ | 13 | 15 | 100 ⁽¹⁰⁰⁾ |
| | $struct_w + prod_w$ | 3 ⁽⁰⁾ | 0 | 3 ⁽³⁾ | 100 ⁽¹⁰⁰⁾ | 100 | 100 | 3 | 6 | 4 | 4 | 4 | 0 | 0 ⁽⁰⁾ | 0 | 33 ⁽¹⁸⁾ |
| Green | $struct_p$ | 1 ⁽⁴⁾ | 12 ⁽⁶⁾ | 5 | 100 | 20 | 1 | 3 | 13 | 2 | 11 | 5 | 28 | 0 | 19 ⁽³¹⁾ | NA |
| | $struct_w$ | 5 | 2 | 40 ⁽⁴⁷⁾ | 100 | 10 | 5 | 8 | 22 | 8 | 11 | 7 | 3 | 9 | 4 ⁽⁵⁾ | NA |
| | $struct_p + prod_p$ | 1 ⁽⁰⁾ | 5 ⁽⁵⁾ | 0 | 72 | 22 | 0 | 19 | 28 | 13 | 36 | 7 | 0 | 20 | 18 ⁽⁴⁾ | 100 ⁽¹⁰⁰⁾ |
| | $struct_w + prod_w$ | 7 | 6 | 6 ⁽⁷⁾ | 98 | 7 | 0 | 7 | 7 | 0 | 2 | 8 | 2 | 0 | 6 ⁽⁶⁾ | 100 ⁽¹⁰⁰⁾ |
| Red | $struct_p$ | 3 | 2 ⁽⁵⁾ | 15 | 100 | 9 | 0 | 0 | 12 | 7 | 8 | 11 | 21 | 0 | 13 | NA |
| | $struct_w$ | 9 | 2 ⁽³⁾ | 27 ⁽⁷⁵⁾ | 100 | 6 | 3 | 9 | 16 | 9 | 15 | 5 | 3 | 34 | 3 ⁽⁵⁾ | NA |
| | $struct_p + prod_p$ | 8 | 0 ⁽⁰⁾ | 2 | 99 | 14 | 8 | 16 | 17 | 8 | 30 | 7 | 14 | 6 | 24 | 100 ⁽¹⁰⁰⁾ |
| | $struct_w + prod_w$ | 16 | 0 ⁽⁰⁾ | 5 ⁽⁵⁾ | 100 | 2 | 6 | 10 | 13 | 13 | 4 | 27 | 0 | 9 | 0 ⁽⁴⁾ | 100 ⁽¹⁰⁰⁾ |

| | | | | | | | | | | | | | | | | |
|----------|---|-------------------|--------------------|--------------------|-----|--------------------|-------------------|--------------------|--------------------|--------------------|--------------------|--------------------|---------------------|--------------------|--------------------|----------------------|
| NIR | struct _p | 3 | 7 ⁽⁶⁾ | 10 | 100 | 3 | 5 | 3 | 3 | 4 | 3 | 0 | 57 | 2 | 14 ⁽²¹⁾ | NA |
| | struct _w | 0 | 12 | 45 | 94 | 30 | 27 | 6 | 8 | 1 | 8 | 1 | 12 | 6 | 9 | NA |
| | struct _p + prod _p | 2 | 23 ⁽¹⁵⁾ | 3 | 97 | 18 | 3 | 11 | 12 | 5 | 3 | 3 | 36 | 3 | 3 ⁽¹⁰⁾ | 100 ⁽¹⁰⁰⁾ |
| | struct _w + prod _w | 0 | 7 | 6 | 100 | 6 | 6 | 6 | 6 | 6 | 0 | 6 | 6 | 0 | 7 | 100 ⁽¹⁰⁰⁾ |
| SWIR-TM5 | struct _p | 16 ⁽³⁾ | 83 | 5 | 48 | 19 | 10 ⁽²⁾ | 43 | 14 | 4 ⁽⁶⁾ | 7 ⁽¹³⁾ | 0 ⁽⁰⁾ | 5 | 34 | 4 ⁽³⁾ | NA |
| | struct _w | 2 ⁽²⁾ | 33 | 15 ⁽²⁷⁾ | 15 | 45 ⁽¹²⁾ | 43 ⁽⁸⁾ | 1 ⁽¹⁾ | 3 ⁽²⁾ | 0 ⁽⁰⁾ | 2 ⁽⁰⁾ | 4 | 12 | 1 ⁽¹⁾ | 15 | NA |
| | struct _p + prod _p | 5 ⁽⁴⁾ | 0 | 4 | 0 | 27 | 6 ⁽⁵⁾ | 11 | 13 | 10 ⁽¹⁶⁾ | 23 ⁽¹⁵⁾ | 0 ⁽⁰⁾ | 0 | 9 | 19 ⁽¹⁹⁾ | 100 ⁽¹⁰⁰⁾ |
| | struct _w + prod _w | 3 ⁽⁰⁾ | 0 | 6 ⁽⁰⁾ | 0 | 7 ⁽⁷⁾ | 0 ⁽²⁾ | 9 ⁽⁵⁾ | 18 ⁽⁴³⁾ | 4 ⁽⁸⁾ | 10 ⁽³⁾ | 10 | 3 | 4 ⁽⁵⁾ | 0 | 100 ⁽¹⁰⁰⁾ |
| SWIR-TM7 | struct _p | 3 ⁽¹⁾ | 8 | 4 ⁽⁴⁾ | 91 | 9 ⁽¹⁴⁾ | 5 ⁽¹⁾ | 5 ⁽²⁾ | 0 | 2 ⁽²⁾ | 18 ⁽⁹⁾ | 22 ⁽²¹⁾ | 0 | 5 ⁽⁴⁾ | 0 | NA |
| | struct _w | 7 ⁽⁸⁾ | 2 | 3 ⁽⁵⁾ | 23 | 5 ⁽⁵⁾ | 6 ⁽⁷⁾ | 14 ⁽¹⁴⁾ | 72 ⁽⁷⁴⁾ | 58 ⁽⁶⁰⁾ | 12 ⁽¹⁹⁾ | 1 | 3 | 0 ⁽⁰⁾ | 3 | NA |
| | struct _p + prod _p | 7 ⁽²⁾ | 5 | 0 ⁽⁷⁾ | 29 | 2 ⁽⁶⁾ | 6 ⁽¹²⁾ | 13 ⁽²⁰⁾ | 0 | 0 ⁽⁰⁾ | 5 ⁽⁴⁾ | 0 ⁽⁰⁾ | 33 | 15 ⁽²⁶⁾ | 0 | 100 ⁽¹⁰⁰⁾ |
| | struct _w + prod _w | 2 ⁽⁰⁾ | 3 | 0 ⁽⁰⁾ | 69 | 10 ⁽¹¹⁾ | 7 ⁽⁷⁾ | 2 ⁽⁰⁾ | 0 ⁽⁰⁾ | 0 ⁽⁰⁾ | 6 ⁽⁶⁾ | 28 | 20 | 6 ⁽⁵⁾ | 7 | 100 ⁽¹⁰⁰⁾ |
| NDVI | struct _p | 4 ⁽⁰⁾ | 52 ⁽⁵⁰⁾ | 50 | 0 | 20 | 6 ⁽¹⁹⁾ | 19 ⁽³⁰⁾ | 0 | 0 | 6 | 69 | 16 ⁽¹⁸⁾ | 23 | 4 ⁽⁴⁾ | NA |
| | struct _w | 0 | 9 ⁽¹⁶⁾ | 32 | 100 | 0 | 9 | 3 | 19 | 7 | 4 | 3 | 100 ⁽⁹⁹⁾ | 3 | 9 ⁽⁸⁾ | NA |
| | struct _p + prod _p | 7 ⁽¹⁰⁾ | 2 ⁽³⁾ | 6 | 99 | 12 | 0 ⁽⁰⁾ | 10 ⁽⁵⁾ | 5 | 2 | 6 | 15 | 0 ⁽⁰⁾ | 2 | 6 ⁽¹⁾ | 100 ⁽¹⁰⁰⁾ |
| | struct _w + prod _w | 21 | 7 ⁽¹⁶⁾ | 2 | 80 | 2 | 16 | 3 | 27 | 11 | 6 | 17 | 3 ⁽⁶⁾ | 15 | 3 ⁽³⁾ | 100 ⁽¹⁰⁰⁾ |

* indicates that mean NDVI was not included in the model.

Appendix B – List of Scientific/Technical Publications

1. Articles in peer-reviewed journals

- Bellis, L. M., A. M. Pidgeon, V. C. Radeloff, V. St-Louis, J. L. Navarro, and M. B. Martella. 2008. Modeling Habitat Suitability for Greater Rheas Based on Satellite Image Texture. *Ecological Applications* **18**:1956-1966.
- Culbert, P. D., A. M. Pidgeon, V. St-Louis, D. Bash, and V. C. Radeloff. 2009. The Impact of Phenological Variation on Texture Measures of Remotely Sensed Imagery. *IEEE Journal of Selected Topics in Applied Earth Observations and Remote Sensing* **2**:299-309.
- St-Louis, V., A. M. Pidgeon, V. C. Radeloff, T. J. Hawbaker, and M. K. Clayton. 2006. High-resolution image texture as a predictor of bird species richness. *Remote Sensing of Environment* **105**:299-312.
- St-Louis, V., A. M. Pidgeon, M. K. Clayton, B. A. Locke, D. Bash, and V. C. Radeloff. 2009. Satellite image texture and a vegetation index predict avian biodiversity in the Chihuahuan Desert of New Mexico. *Ecography* **32**:468-480.
- St-Louis, V., A. M. Pidgeon, M. K. Clayton, B. A. Locke, D. Bash, and V. C. Radeloff. 2010. Habitat variables explain Loggerhead Shrike occurrence in the northern Chihuahuan Desert, but are poor correlates of fitness measures. *Landscape Ecology* **25**:643-654.
- St-Louis, V., M. K. Clayton, A. M. Pidgeon, and V. C. Radeloff. An evaluation of the influence of priors on the predictive ability of Bayesian model averaging. *in review*; *Oecologia*.
- St-Louis, V., A. M. Pidgeon, M. K. Clayton, B. A. Locke, D. Bash, and V. C. Radeloff. Predicting species distribution across heterogeneous habitats. *Submitted* to *Journal of Wildlife Management*.

2. Technical Reports

None

3. Conference or symposium proceedings scientifically recognized and referenced.

None

4. Conference or symposium abstracts.

2010. Wood, E. M., A. M. Pidgeon, and V. C. Radeloff. Evidence for Karner Blue Butterfly (*Lycaeides melissa samuelis*) as a Surrogate Species for the Conservation of Oak Savanna Bird Community Assemblages. 24th International Congress for Conservation Biology, Edmonton, AB. 3-7 July 2010.
2010. Wood, E. M., A. M. Pidgeon, and V. C. Radeloff. The use of image texture as a tool for predicting bird habitat. COS/AOU/SCO. San Diego, CA. 7-11 February 2010.

2009. Culbert, P., V. St.-Louis, A. M. Pidgeon, and V. C. Radeloff. 2009. Modeling avian richness patterns with texture measures of remotely sensed imagery. American Geophysical Union Fall Meeting, San Francisco, California. 14 – 18 December 2009.
2008. St-Louis, V. A. M. Pidgeon, and V. C. Radeloff. At which scale does habitat heterogeneity matter for avian biodiversity? A case study for the Loggerhead Shrike in the Chihuahuan Desert of New Mexico. US-International Association of Landscape Ecology Symposium. Madison, WI. 6-10 April 2008.
2008. P. D. Culbert, V. St-Louis, D. Bash, A. M. Pidgeon, and V. C. Radeloff. Evaluating the impact of phenological variation on texture measures of remotely-sensed imagery. US-International Association of Landscape Ecology Symposium. Madison, WI. 6-10 April 2008.
2008. Wood, E. M., A. M. Pidgeon, and V. C. Radeloff. Factors affecting avian use and occupancy of savanna habitats at Fort McCoy, WI. 4th International Partners in Flight Conference. McAllen TX. 13-16 February 2008.
2007. Wood, E. M. , A. M. Pidgeon, and V. C. Radeloff. The potential of image texture for predicting avian species richness in a Midwest savanna. 68th Midwest Fish and Wildlife Conference. Madison, WI. 9-12 December 2007.
2007. St-Louis, V., A. M. Pidgeon, V. C. Radeloff. Image texture and vegetation indices as predictors of bird species richness in the Chihuahuan Desert. International Association of Landscape Ecology, Tuscon Arizona. 10 April, 2007.
2006. Bellis, L. M., A. M. Pidgeon, V. C. Radeloff, J. L. Navarro, and M. B. Martella. Modelling habitat suitability of greater rheas (*Rhea americana*) in a grassland relict of central Argentina. The 7th International Conference for the Management of Wildlife in Amazonia and Latin America, Ilheus, Brasil. 4 September 2006.
2006. St-Louis, V. A. M. Pidgeon, and V.C. Radeloff. Texture measures in digital orthophotos as predictors of bird species richness in semi-arid environments. Association of American Geographers, Chicago, IL. 7 March 2006.

5. Text books or book chapters.

None